

AD _____

Award Number: DAMD17-03-1-0092

TITLE: Prostate Cancer Skeletal Metastases: Pathobiology and Interventions

PRINCIPAL INVESTIGATOR: Evan T. Keller, Ph.D.

CONTRACTING ORGANIZATION: University of Michigan
Ann Arbor, MI 48109

REPORT DATE: February 2004

TYPE OF REPORT: Annual

PREPARED FOR: U.S. Army Medical Research and Materiel Command
Fort Detrick, Maryland 21702-5012

DISTRIBUTION STATEMENT: Approved for Public Release;
Distribution Unlimited

The views, opinions and/or findings contained in this report are those of the author(s) and should not be construed as an official Department of the Army position, policy or decision unless so designated by other documentation.

20040706 020

REPORT DOCUMENTATION PAGEForm Approved
OMB No. 074-0188

Public reporting burden for this collection of information is estimated to average 1 hour per response, including the time for reviewing instructions, searching existing data sources, gathering and maintaining the data needed, and completing and reviewing this collection of information. Send comments regarding this burden estimate or any other aspect of this collection of information, including suggestions for reducing this burden to Washington Headquarters Services, Directorate for Information Operations and Reports, 1215 Jefferson Davis Highway, Suite 1204, Arlington, VA 22202-4302, and to the Office of Management and Budget, Paperwork Reduction Project (0704-0188), Washington, DC 20503

1. AGENCY USE ONLY (Leave blank)		2. REPORT DATE February 2004	3. REPORT TYPE AND DATES COVERED Annual (1 Feb 2003 - 31 Jan 2004)	
4. TITLE AND SUBTITLE Prostate Cancer Skeletal Metastases: Pathobiology and Interventions			5. FUNDING NUMBERS DAMD17-03-1-0092	
6. AUTHOR(S) Evan T. Keller, Ph.D.				
7. PERFORMING ORGANIZATION NAME(S) AND ADDRESS(ES) University of Michigan Ann Arbor, MI 48109 E-Mail: etkeller@umich.edu			8. PERFORMING ORGANIZATION REPORT NUMBER	
9. SPONSORING / MONITORING AGENCY NAME(S) AND ADDRESS(ES) U.S. Army Medical Research and Materiel Command Fort Detrick, Maryland 21702-5012			10. SPONSORING / MONITORING AGENCY REPORT NUMBER	
11. SUPPLEMENTARY NOTES				
12a. DISTRIBUTION / AVAILABILITY STATEMENT Approved for Public Release; Distribution Unlimited			12b. DISTRIBUTION CODE	
13. ABSTRACT (Maximum 200 Words) Prostate cancer skeletal metastases are considered osteoblastic; however, histopathological examination usually reveals underlying osteoclastic activity. A key molecule required for induction of osteoclastic activity is receptor activator of NFkB ligand (RANKL). RANKL activity is opposed by osteoprotegerin (OPG). Thus, the balance of RANKL and OPG in the prostate cancer tissue may regulate the overall phenotype of the metastatic lesion. We are testing the hypothesis that an increase in the RANKL:OPG ratio contributes to the development of CaP skeletal metastases and a corollary hypothesis is that restoring the RANKL:OPG axis through inhibition of RANKL activity will diminish progression of skeletal metastases. In this report, we summarize our work that demonstrates blocking RANKL with sRANK-Fc diminishes progression of human prostate cancer in human bone implanted in mice. Additionally, we demonstrate that the RANKL promoter is active in bone and induced by transforming growth factor-beta (TGF-beta).				
14. SUBJECT TERMS Skeletal Metastasis; Bone remodeling; osteoclastogenesis, gene regulation			15. NUMBER OF PAGES 25	
			16. PRICE CODE	
17. SECURITY CLASSIFICATION OF REPORT Unclassified	18. SECURITY CLASSIFICATION OF THIS PAGE Unclassified	19. SECURITY CLASSIFICATION OF ABSTRACT Unclassified	20. LIMITATION OF ABSTRACT Unlimited	

NSN 7540-01-280-5500

Standard Form 298 (Rev. 2-89)
Prescribed by ANSI Std. Z39-18
298-102

Table of Contents

Cover.....	1
SF 298.....	2
Table of Contents.....	3
Introduction.....	4
Body.....	4
Key Research Accomplishments.....	5
Reportable Outcomes.....	6
Conclusions.....	6
References.....	none
Appendices.....	7

INTRODUCTION:

Prostate cancer skeletal metastases are considered osteoblastic; however, histopathological examination usually reveals underlying osteoclastic activity. A key molecule required for induction of osteoclastic activity is receptor activator of NF κ B ligand (RANKL). RANKL activity is opposed by osteoprotegerin (OPG). Thus, the balance of RANKL and OPG in the prostate cancer tissue may regulate the overall phenotype of the metastatic lesion. We have determined that prostate cancer cells express increasing levels of RANKL and decreasing levels of OPG. Additionally, we have determined that androgen promotes OPG expression at the transcriptional level. Thus, loss of androgen, may reduce OPG expression and favor a shift towards RANKL activity. Additionally, in a murine model, we have demonstrated the ability to inhibit establishment of prostate cancer in bone by blocking RANKL-induced osteoclastic activity using OPG. However, OPG can bind pro-apoptotic molecules and block apoptosis of cancer cells. Thus, it may not be useful for clinical use. Instead, alternative methods to block RANKL activity may be more clinically relevant. Based on our previous findings and those of others our hypothesis is that an increase in the RANKL:OPG ratio contributes to the development of CaP skeletal metastases. Accordingly, a corollary hypothesis is that restoring the RANKL:OPG axis through inhibition of RANKL activity will diminish progression of skeletal metastases. Accordingly, the specific aims of this project are to (1) identify the mechanisms through which OPG expression is regulated in CaP cells and (2) determine if inhibition of RANKL activity by methods other than OPG can block the establishment and progression of CaP skeletal metastases in vivo.

BODY:

Original Tasks:

Task 1. Identify the mechanisms through which OPG expression are regulated in CaP cells (Months 1-24):

- a. Determine OPG promoter activity in other CaP cells (Months 1-6).
 - i. Transfect cells with OPG promoter reporter and treat with dihydrotestosterone.
- b. Define cis-acting sites that are responsible for activation and androgen response of the OPG promoter in CaP cells (Months 7-24).
 - i. Transfect cells with serially deleted OPG promoter-reporter vectors (Months 7-10).
 - ii. Create and characterize activity of 50 bp deletion mutants based on information from Task 1bi (Months 11-14).
 - iii. Clone into reporter vector and characterize activity of 50 bp fragment (from Task 1bii) (Months 15-19).
 - iv. Create and characterize activity of point-mutated 50 bp fragment (Months 20-24).

Task 2. Determine if inhibition of RANKL activity by methods other than OPG can block the establishment and progression of CaP skeletal metastases in vivo (Months 12-36).

- a. Evaluate effect of sRANK on prostate cancer establishment in bone (Months 12-17)
- b. Evaluate effect of sRANK on prostate cancer progression in bone (Months 18-24)
- c. Determine effect of anti-RANKL antibody on prostate cancer establishment in bone (Months 25-30)
- d. Determine effect of anti-RANKL antibody on prostate cancer progression in bone (Months 31-36).

Overall, we have reversed the order of the tasks so that we are now performing the bulk of Task 2 first; however, we have made some progress on Task 1.

Task 1:

We have five different lengths of the OPG promoter.

We have identified that dihydrotestosterone (DHT) at 50 nM generally inhibits the OPG promoter, but at 100 nM it induces the OPG promoter. This is reminiscent of the biphasic response seen with PSA and DHT, which first induces PSA, then inhibits PSA production.

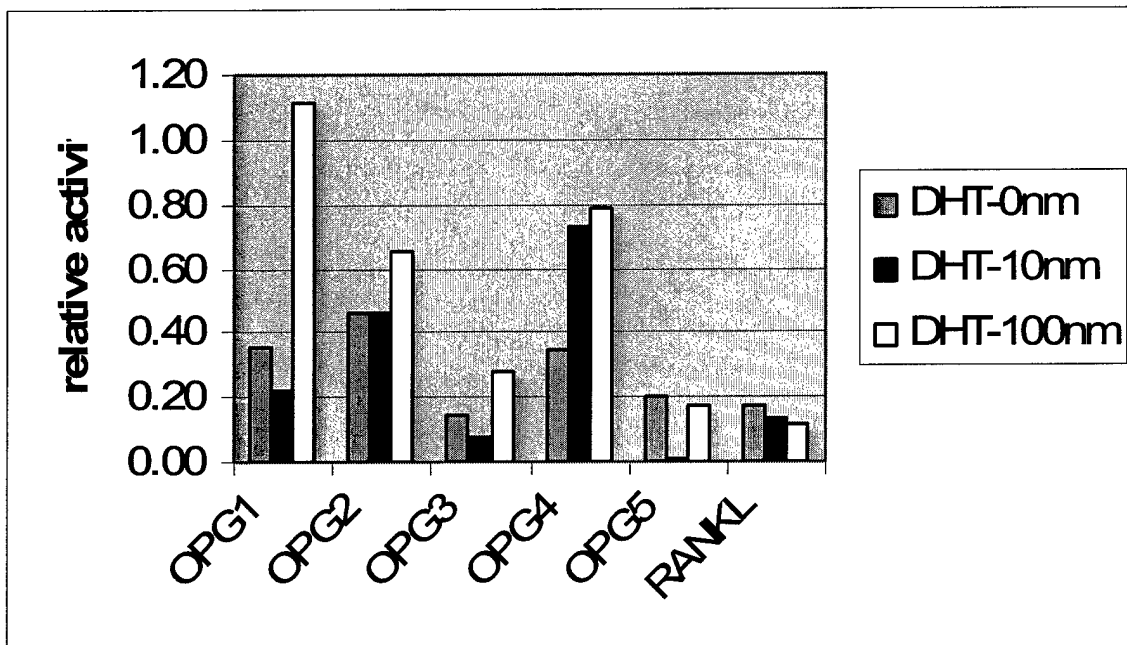


Fig. 1 C4-2B prostate cancer cells were transfected with the OPG promoter constructs of different length and treated with the indicated level of DHT. Twenty-four hours later total cell lysate was collected for measurement of luciferase.

Task 2:

We have identified that sRANK-Fc inhibits progression of prostate cancer progression in bone. This work is presented in the attached Cancer Research publication #1. Additionally, we have extended these studies to delineate how RANKL expression is regulated in bone. We identified that the RANKL promoter is activated in bone by transforming growth factor-beta. This work is presented in the attached Prostate publication #2.

KEY RESEARCH ACCOMPLISHMENTS:

- Demonstration that DHT regulates OPG in a biphasic fashion.
- Demonstration that sRANK-Fc can inhibit prostate cancer growth in bone but not soft tissue.
- Demonstration of RANKL gene promoter activity in vivo.
- Demonstrate that TGF-beta, a factor produced upon resorption of bone, induces the RANKL promoter.
- Demonstrate that tumor volume measured in vivo by bioluminescence imaging correlates with tumor volume measured by PSA.

REPORTABLE OUTCOMES:

1. MANUSCRIPTS

Zhang J, Dai J, Yao Z, Lu Y, Dougall W, Keller ET. Soluble RANK-Fc diminishes prostate cancer progression in bone. *Cancer Res.* 63:7883-7890, 2003.

Zhang J, Lu Y, Kitazawa R, Kitazawa S, Dai J, Zhao X, Yao Z, Pienta KJ, Keller ET. In Vivo Real-Time Imaging of TGF- β -Induced Transcription Activation of the RANK Ligand Gene Promoter in Intraosseous Prostate Cancer

CONCLUSIONS:

RANKL promotes prostate cancer growth in bone. Blocking RANKL is an effective strategy to diminish progression of prostate cancer growth in bone. Most likely it works through inhibiting osteoclastogenesis as the inhibitory effect is specific to tumor growing in bone as opposed to subcutaneous tumor.

Additionally, the bone environment may promote RANKL expression from tumor cells through release of factors that increase RANKL expression such as TGF- β , which we demonstrated. This suggests there is a vicious cycle present that allows for increased bone resorption, release of prostate cancer-active growth factors, which in turn stimulates prostate cancer cells to continue growth and effect bone remodeling. This may be tempered in the bone environment by production of OPG which is regulated by androgens. However, at physiological levels, it appears that DHT inhibits OPG production, which would help contribute to the overall osteolytic activity.

Appendix Cover Sheet

Soluble Receptor Activator of Nuclear Factor κ B Fc Diminishes Prostate Cancer Progression in Bone

Jian Zhang,¹ Jinlu Dai,² Zhi Yao,⁴ Yi Lu,⁴ William Dougall,⁵ and Evan T. Keller^{1,2,3}

¹Department of Pathology and ²Unit for Laboratory Animal Medicine, School of Medicine, and ³Connective Tissue Oncology Program, Comprehensive Cancer Center, University of Michigan, Ann Arbor, Michigan; ⁴Department of Immunology, Tianjin Medical University, Tianjin, China; and ⁵Department of Cancer Biology, Amgen, Seattle, Washington

ABSTRACT

Prostate cancer (CaP) develops metastatic bone lesions that consist of a mixture of osteosclerosis and osteolysis. We have previously demonstrated that targeting receptor activator of nuclear factor κ B ligand (RANKL) with osteoprotegerin (OPG) prevents the osteolytic activity of CaP and its ability to establish tumor in bone. However, OPG can block tumor necrosis factor-related apoptosis-inducing ligand (TRAIL)-mediated apoptosis, suggesting that the clinical use of OPG may prevent apoptosis of tumors mediated by TRAIL. Thus, methods to block RANKL activity, other than OPG, may be important. Accordingly, we evaluated the ability of soluble murine RANK-Fc (sRANK-Fc) to prevent progression of established CaP in a severe combined immunodeficient mouse implanted with fetal human bone. We first confirmed that sRANK did not block TRAIL-mediated apoptosis of LuCaP cells *in vitro* and that it did block LuCaP-conditioned media-induced osteoclastogenesis *in vitro*. Then, LuCaP 35 CaP cells were injected into the marrow space of the bone implanted in the severe combined immunodeficient mice implanted with fetal human bone and allowed to develop into tumors for 6 weeks. Either vehicle or sRANK-Fc was then administered for 6 weeks. sRANK-Fc diminished tumor-induced osteoblastic lesions as demonstrated by radiograph, bone mineral density measurement, and bone histomorphometry. sRANK-Fc also reduced systemic bone remodeling markers, including serum osteocalcin and bone-specific alkaline phosphatase and urine N-telopeptide of collagen. Finally, sRANK-Fc decreased serum prostate-specific antigen levels and tumor volume in the bone, which indicates decreased tumor burden. In contrast, sRANK-Fc had no effect on s.c. implanted LuCaP cells. We conclude that sRANK-Fc is an effective inhibitor of RANKL that diminishes progression of CaP growth in bone through inhibition of bone remodeling.

INTRODUCTION

The skeleton is the most common site of CaP⁶ metastasis, with up to 84% of patients demonstrating skeletal metastases (1). Although characterized radiographically as primarily osteoblastic, it is recognized that CaP skeletal metastases have an extensive bone resorptive component (2, 3). The tumor-induced bone resorption is primarily caused by osteoclasts (4), which accounts for the ability of antiosteoclastogenic agents, such as bisphosphonates that induce osteoclast apoptosis, to diminish tumor-induced osteolysis, decrease pain, and improve mobility in CaP skeletal metastasis patients (5).

Received 6/5/03; revised 8/8/03; accepted 9/3/03.

Grant support: Grants from the Army Medical Research and Materiel Command Prostate Cancer Research Program (DAMD17-03-1-0092), National Cancer Institute Specialized Programs of Research Excellence (1 P50 CA69568), University of Michigan Cancer Center Support (5 P30 CA46592), and University of Michigan Program of Comparative Integrative Genomics.

The costs of publication of this article were defrayed in part by the payment of page charges. This article must therefore be hereby marked *advertisement* in accordance with 18 U.S.C. Section 1734 solely to indicate this fact.

Requests for reprints: Evan T. Keller, Room 5304 Cancer Center and Geriatrics Center Building, Box 0940, 1500 East Medical Center Drive, Ann Arbor, MI 48109-0940. Phone: (734) 615-0280; Fax: (734) 936-9220; E-mail: etkeller@umich.edu.

⁶The abbreviations used are: CaP, prostate cancer; TNF, tumor necrosis factor; NF- κ B, nuclear factor κ B; RANKL, receptor activator of NF- κ B ligand; BV/TV, trabecular volume:total bone volume; OPG, osteoprotegerin; TRAIL, tumor necrosis factor-related apoptosis-inducing ligand; CRD, cysteine-rich domain; SCID, severe combined immunodeficient; PSA, prostate-specific antigen; TRAP, tartrate-resistant acid phosphatase; DEXA, dual-energy X-ray absorptiometry; BMD, bone mineral density; BAP, bone-specific alkaline phosphatase; OC, osteocalcin; FBS, fetal bovine serum; CM, conditioned media; NTx, N-telopeptide.

Osteoclastogenesis is regulated by a cytokine system consisting of the TNF family member RANKL (also called OPGL, TRANCE, and ODF), its receptor RANK (also called ODAR), and its decoy receptor OPG (also called OCIF and TR1; reviewed in Ref. 6). RANKL, a transmembrane molecule located on bone marrow stromal cells and osteoblasts, binds to RANK, which is located on the surface of osteoclast precursors. This ligand-receptor interaction activates NF κ B, which stimulates differentiation of osteoclast precursors to osteoclasts. OPG, also produced by osteoblasts/stromal cells, binds to RANKL, sequestering it from binding to RANK, which results in inhibition of osteoclastogenesis.

We have previously shown that RANKL mediates CaP-induced osteoclastogenesis (7). Furthermore, administration of OPG prevented the establishment of CaP tumor injected into murine bone. These results suggest that blocking RANKL may prevent progression of CaP in bone. However, OPG has been demonstrated to bind the TNF receptor TRAIL and block TRAIL-mediated apoptosis in cancer cells (8, 9). Clinical evidence for the importance of TRAIL-mediated apoptosis is suggested by the observation that TRAIL receptor expression is associated with apoptosis of hepatoma cells (10). Furthermore, TRAIL is considered to be a promising anticancer agent (11, 12). Taken together, these observations suggest that therapeutic use of OPG in clinical cancer may not be prudent because of its potential to protect tumor cells from apoptosis. Thus, development of alternative methods to block RANKL that do not interact with TRAIL may provide useful therapies to prevent CaP progression in bone.

Recently, the use of a sRANK-Fc, which blocks RANKL, was demonstrated to inhibit both lung carcinoma and multiple myeloma-induced bone resorption (13, 14). sRANK-Fc is a chimeric protein formed by fusing the four CRDs of RANK with the Fc portion of human IgG1 (14). The two disulfide bonds of the Fc portion allow homodimerization of the sRANK-Fc proteins, resulting in a homodimer with eight CRDs, which are believed to be responsible for binding to RANKL. The sRANK differs from OPG, which also binds to RANKL, because in addition to containing four CRDs, OPG also has two death domains and a heparin-binding domain (14). These differences in structure between OPG and sRANK-Fc result in different functions between these two molecules including the inability of sRANK-Fc to bind TRAIL. The inability to block TRAIL-mediated apoptosis, yet bind RANKL, suggests that sRANK-Fc may be a useful molecule to prevent progression of CaP in bone. Accordingly, in the current study, we investigated the ability of sRANK-Fc to block the progression of CaP in human bone implanted in a mouse.

MATERIALS AND METHODS

Animals. Male SCID mice (Charles River, Wilmington, MA), 6 weeks of age, were housed under pathogen-free conditions in accordance with the NIH guidelines using an animal protocol approved by the University of Michigan Animal Care and Use Committee.

sRANK-Fc. The sRANK-Fc used in these studies was provided by Amgen Inc. (Seattle, WA) and contains the murine extracellular domain of RANK (through Pro213) fused to human IgG1 Fc. The RANK-Fc protein was produced in Chinese hamster ovary cells as described previously (13, 15).

Preparation of Single-Cell Suspension. LuCaP 35, kindly provided by Dr. Robert Vessella (University of Washington, Seattle, WA), is an androgen-

sensitive, PSA-producing human CaP xenograph derived from the lymph nodes of a patient that had failed androgen-deprivation therapy (16, 17). Single-cell suspensions of LuCaP 35 were prepared by resecting the s.c. xenografts and cutting them into small pieces in HBSS with 1% FBS. The small pieces were then rubbed gently between frosted glass slides to obtain single-cell suspensions in HBSS containing 1% FBS. RBCs were lysed with ammonium chloride solution (StemCell Technologies Inc., Vancouver, British Columbia, Canada) and centrifuged at $300 \times g$ for 10 min in HBSS with 1% FBS, and the cell pellet was resuspended in RPMI 1640 with 10% FBS. Cell viability was determined by trypan blue counting, and only preparations with >90% viability were used for *in vivo* injection.

Obtaining CM. CM were obtained from cells as described previously (7). Briefly, 5×10^6 cells were plated in 10-cm tissue culture dishes for 12 h in RPMI 1640 with 10% FBS. The media were then changed to 10 ml of RPMI plus 0.5% FBS, and supernatants were collected 24 h later. To normalize for differences in cell density because of proliferation during the culture period, cells from each plate were collected and total DNA content/plate was determined (spectrophotometric absorbance, 260 nm). CM were then normalized for DNA content between samples by adding RPMI.

Treatment. Forty SCID mice had half-sections of human fetal bone (cut in half longitudinally) implanted s.c. as described previously (18). Four weeks later, LuCaP 35 CaP cells (3×10^5 in 50 μ l of RPMI 1640 with 10% FBS) were injected into the marrow space of the implanted bone, and tumors were allowed to develop. Six weeks after LuCaP 35 implant, mice were palpated for presence of tumors, which grows out of the open marrow cavity of the bone, and blood was collected and measured for PSA levels (28 of 40 mice had palpable evidence of tumors and were positive for PSA). The mice with tumors were then divided randomly into three groups ($n = 9$ /group) to be either immediately sacrificed (basal) or receive either sRANK-Fc (200 μ g/mouse) or saline vehicle by i.p. injection three times per week based on a previous study (19). Mice were sacrificed after 6 weeks of sRANK administration. An additional group of mice ($n = 10$) to serve as a control group received bone implants, and 4 weeks after implant (at the same time as the treatment groups received tumor), 50 μ l of RPMI with 10% FBS were injected into the marrow cavity, and these mice were sacrificed 6 weeks after injection (in parallel with the basal group). Serum, urine, and bones were collected for evaluation. Before sacrifice, the animals were anesthetized, and magnified flat radiographs were taken with a Faxitron (Faxitron X-Ray Corp., Wheeling, IL).

Histopathology and Bone Histomorphometry. Histopathology was performed as described previously (7). Briefly, bone specimens were fixed in 10% formalin for 24 h, then decalcified using 12% EDTA for 72 h. The specimens were then paraffin embedded, sectioned (5 μ m), and stained with H&E to assess histology or stained with TRAP to identify osteoclasts. Four discontinuous random regions of interest were examined within each bone implant to represent the bone fragment. To perform TRAP staining, nonstained sections were deparaffinized and rehydrated, then stained for TRAP (acid phosphatase kit, model 387-A; Sigma Diagnostics, St. Louis, MO) as directed by the manufacturer with minor modification. Briefly, the specimens were fixed for 30 s and then stained with acid phosphatase and tartrate solution for 1 h at 37°C, followed by counterstaining with hematoxylin solution. Osteoclasts were determined as TRAP-positive staining multinuclear (>3 nuclei) cells by light microscopy. Histomorphometric analysis was performed on a BIOQUANT system (R&M Biometrics, Inc., Nashville, TN) as described previously (20). The terminology used was that recommended by the Histomorphometry Nomenclature Committee of the American Society for Bone and Mineral Research (21). Tumor area was determined as the proportion of tumor area in the total nonmineralized portion of the bone.

DEXA Measurement and X-Ray. BMD of the excised bone implants was measured using DEXA on an Eclipse Peripheral DEXA Scanner using pDEXA Sabre software, version 3.9.4, in research mode (Norland Medical Systems, Fort Atkinson, WI). Excised implants were scanned at 2 mm/s with a resolution of 0.1×0.1 mm. Three 0.5-cm regions of interest were selected randomly for each fragment to determine BMD. Short-term BMD precision (percentage of coefficient of variation) was ~3% for this technique. Radiographs were taken before the sacrifice of the animals and after the excision of bone implants by using a Faxitron.

PSA Measurement. Total PSA levels in serum were determined using the Accucyte Human PSA assay (Cytimmune Sciences Inc., College Park, MA). The sensitivity of this assay is 0.488 mg/ml.

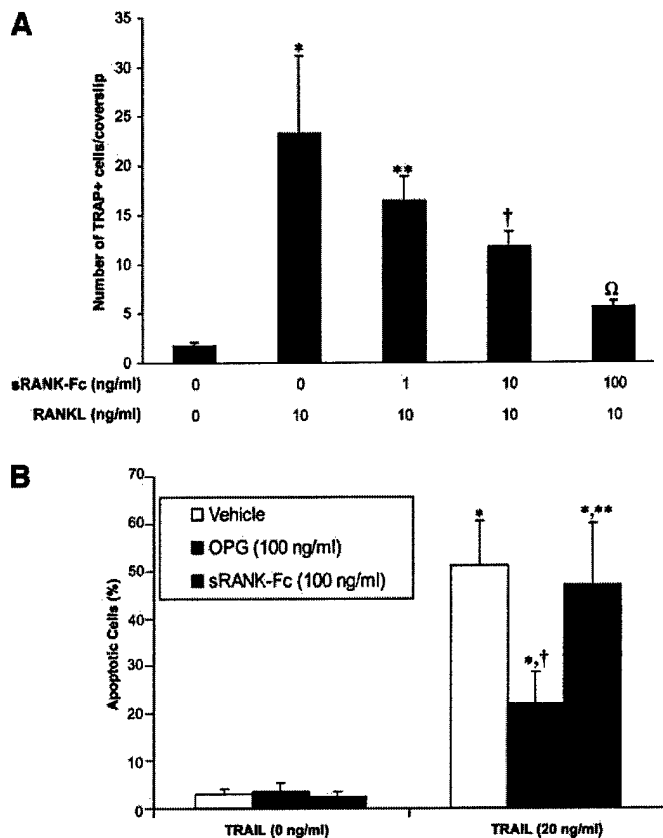


Fig. 1. Effect of sRANK-Fc on RANKL activity and TRAIL-mediated apoptosis *in vitro*. A, single-cell suspensions of RAW 264.7 cells were plated in 24-well plates (1×10^5 cells/well) on top of sterile coverslips in RPMI plus 10% FBS. Cells were grown for 12 h, then the media were changed to RPMI plus 0.5% FBS, and recombinant human sRANKL (10 ng/ml) and sRANK-Fc were added as indicated. Osteoclasts were identified as TRAP-positive multinucleated (>3 nuclei) cells, and the number of osteoclasts per coverslip were quantified. Data are reported as the mean \pm SD of triplicates from two independent experiments. *, $P < 0.001$ compared with nontreatment culture; **, $P < 0.05$ compared with the RANKL only treatment; †, $P < 0.01$ compared with RANKL only and $P < 0.05$ compared with 1 ng/ml sRANK-Fc treatment; Ω, $P < 0.01$ compared with RANKL only and 10 ng/ml sRANK-Fc treatments (one-way ANOVA and Fisher's protected least significant difference for *post hoc* analysis). B, LuCaP cells were plated (1×10^5 cells/well) in 12-well plates in RPMI plus 10% FBS. After 12 h of culture, media were changed to RPMI plus 0.5% FBS, and OPG, sRANK-Fc, or TRAIL was added as indicated. After an additional 24 h of culture, cells were assessed for apoptosis on a fluorescent microscope using Annexin V-FITC staining. Results are reported as the mean \pm SD of two experiments. *, $P < 0.01$ compared with no TRAIL for each respective compound; †, $P < 0.01$ compared with TRAIL-treated vehicle group; **, $P < 0.01$ compared with TRAIL-treated OPG group (ANOVA and Fisher's protected least significant difference for *post hoc* analysis).

Serum OC Measurement. Serum human OC was measured by a competitive immunoassay kit (Metra Osteocalcin, Quidel Corporation, Santa Clara, CA). The assay does not cross-react with murine OC. This antibody is conformationally dependent and recognizes only intact (*de novo*) OC and not fragments from resorbed bone tissues. The sensitivity of this assay is 0.45 ng/ml.

Serum BAP Measurement. Serum human BAP was measured by an immunoassay kit (Metra BAP ELA, Quidel Corporation, Santa Clara, CA). This assay does not cross-react with murine BAP. The sensitivity of this assay is 0.7 units/liter.

Urine NTx and Creatinine Measurements. Urine NTx was measured using human-specific ELISA, as recommended by the manufacturer (Osteomark NTx; Ostex Inc.). Results were reported as a ratio of NTx bone collagen equivalents (nanomolar bone collagen equivalents) to urine creatinine (millimole creatinine). Urine creatinine was measured using a creatinine kit (Metra Biosystems, Mountain View, CA) as directed by the manufacturer.

Cell Viability. Single-cell suspension of LuCaP cells were plated at 2×10^6 /plate in 60-mm plates in triplicates with RPMI and 10% FBS. After 12 h of culture, media were changed to RPMI plus 0.5% FBS and sRANK-Fc

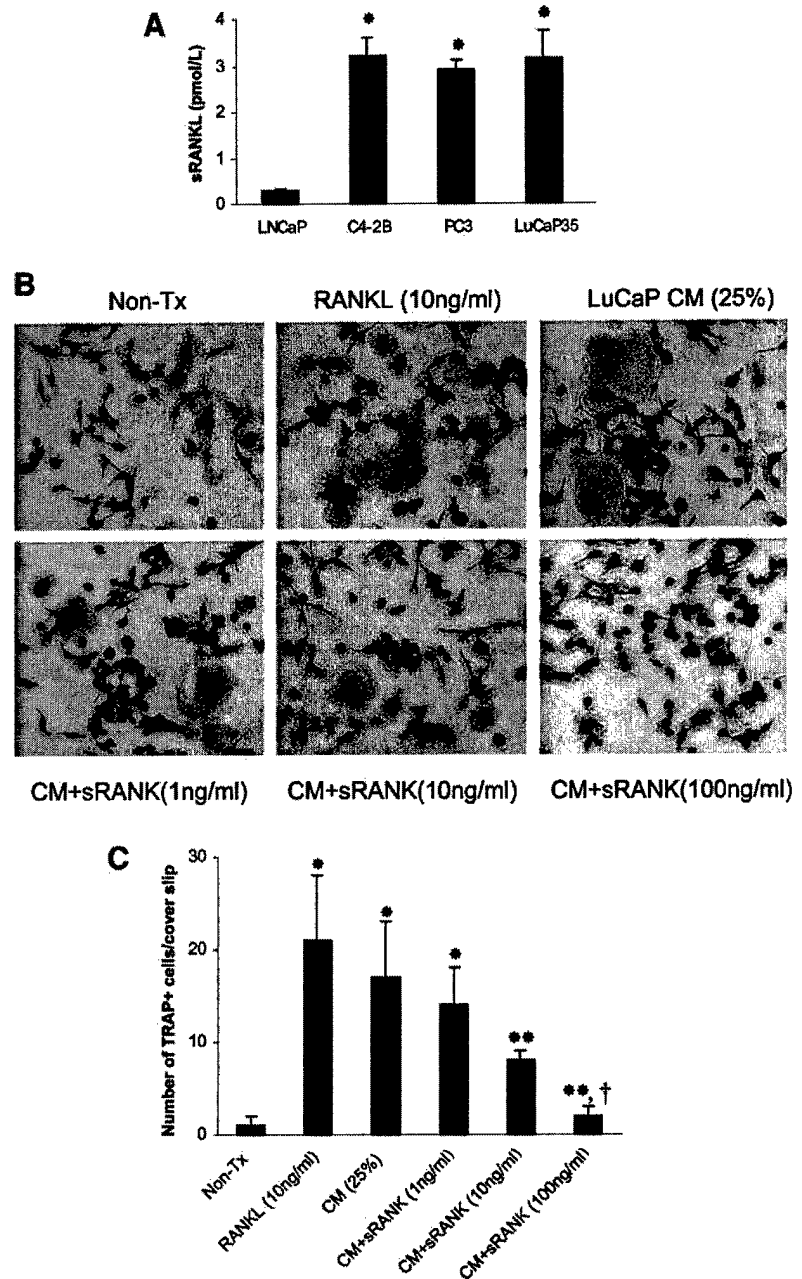


Fig. 2. Effects of sRANK-Fc on CaP-induced osteoclast activity *in vitro*. **A**, LNCaP, C4-2B, PC3, and LuCaP 35 cells were plated (5×10^5 cells) in 12-well plates. After 24 h, CM were collected and subjected high-sensitivity ELISA for sRANKL. Data are reported as the mean \pm SD of three experiments. *, $P < 0.05$ compared with LNCaP (one-way ANOVA and Fisher's protected least significant difference for *post hoc* analysis). **B**, representative pictures of cultures stained for TRAP. Single-cell suspensions of RAW 264.7 cells were plated in 24-well plates (1×10^5 cells/well) on top of sterile coverslips in RPMI plus 10% FBS. Cells were grown for 12 h, then the media were changed to RPMI plus 0.5% FBS. Either recombinant human sRANKL (10 ng/ml) or CM harvested (as described in "Materials and Methods") from LuCaP cells was added to a final concentration of 25% (vol/vol) as indicated. Immediately, the indicated concentration of sRANK-Fc was added. Osteoclasts were identified as TRAP-positive multinucleated (>3 nuclei) cells. **C**, number of osteoclasts per coverslip were quantified. Data are reported as the mean \pm SD of quadruplicates from two independent experiments. *, $P < 0.001$ compared with nontreatment culture; **, $P < 0.05$ compared with the CM-treated culture and 1 ng/ml treatment; †, $P < 0.01$ compared with 10 ng/ml treatment (one-way ANOVA and Fisher's protected least significant difference for *post hoc* analysis).

was added at different concentrations, and 24 h after an additional 24 h, cells were collected and viability was examined by trypan blue exclusion.

Cell Proliferation. Cell proliferation was measured using the CellTiter 96 AQ Non-radioactive cell proliferation assay (Promega, Madison, WI). Briefly, LuCaP cells in RPMI plus 5% FBS were added to the wells of a 96-well plates at 5000/well in triplicates. After 12 h of culture, the media were changed to RPMI plus 0.5% FBS, and a different concentration of sRANK-Fc was added. Cells were allowed to grow for 24 h, then 20 μ l/well of combined MTS/PMS solution were added. After incubation of 1 h at 37°C in a humidified 5% CO₂ atmosphere, the absorbance at 490 nm was recorded by using an ELISA plate reader.

Cell Apoptosis. LuCaP cells were plated at 1×10^6 /well in 12-well plates on sterile coverslips in triplicate with RPMI plus 10% FBS. After 12 h of culture, media were changed to RPMI plus 0.5% FBS and immediately a different concentration of recombinant OPG (R&D Systems Inc.), sRANK-Fc, or TRAIL (R&D Systems, Inc.) was added. Subsequently, cells were evaluated for apoptosis on a fluorescent microscope using Annexin V-FITC detection kit (PharMingen, San Diego, CA) following the manufacturer's protocol. Ten

random $\times 50$ fields were counted, and the results are reported as percentage of FITC-positive cells.

Statistical Analysis. Statistical analysis was performed using Statview software (Abacus Concepts, Berkeley, CA). ANOVA was used for initial analyses, followed by Fisher's protected least significant difference for *post hoc* analyses. Differences with a $P < 0.05$ were determined as statistically significant.

RESULTS

RANKL is a key inducer of osteoclastogenesis. To ensure that sRANK-Fc blocks RANKL-induced osteoclastogenesis *in vitro*, we cocultured osteoclast precursor RAW cells with RANKL in the presence of increasing doses of sRANK-Fc. RANKL-induced osteoclastogenesis and sRANK-Fc inhibited the osteoclastogenesis in a dose-responsive fashion (Fig. 1A). OPG has been shown to bind TRAIL (22) and block TRAIL-mediated apoptosis in CaP cells *in*

in vitro (9), which suggests that it may be protect cancer cells against TRAIL-mediated apoptosis *in vivo*. Accordingly, other factors to block RANKL that do not block the proapoptotic activity of TRAIL may be useful for cancer therapy. We have determined that sRANK-Fc does not bind TRAIL (data not shown); however, to ensure that it does not block TRAIL-mediated apoptosis, we tested the effect of sRANK-Fc on TRAIL-mediated apoptosis of LuCaP cells. We found that although OPG diminished TRAIL-mediated apoptosis of LuCaP cells, sRANK-Fc had no effect (Fig. 1B). These data demonstrate that sRANK-Fc blocks RANKL-induced osteoclastogenesis but does not protect LuCaP cells against TRAIL-mediated apoptosis.

To determine whether LuCaP 35 cells produce sRANKL, we created single-cell suspensions of LuCaP 35 and grew them for 24 h, then collected the culture supernatants to test for sRANKL expression. LuCaP 35 cells secreted sRANKL at levels similar to C4-2B and PC-3 CaP cells, but ~8-fold higher levels than LNCaP CaP cells (Fig. 2A). To determine whether sRANK-Fc could inhibit LuCaP-induced osteoclastogenesis, we incubated osteoclast precursor RAW cells with LuCaP CM in the absence and presence of sRANK-Fc. LuCaP CM induced osteoclasts, and sRANK-Fc decreased LuCaP-mediated osteoclastogenesis in a dose-responsive fashion (Fig. 2, B and C). These data demonstrate that LuCaP35 produces functional sRANKL and that LuCaP-induced osteoclastogenesis can be inhibited by sRANK-Fc.

To evaluate the ability of sRANK-Fc to prevent progression of established CaP in bone, we s.c. implanted human fetal bone into 40 SCID mice. Four weeks later, LuCaP 35 CaP cells were injected into the marrow space of the implanted bone and allowed to develop into tumors. Six weeks after tumor implant, mice were palpated for presence of tumors. We determined that 28 of 40 mice had palpable evidence of tumor growth in the implanted bone (70% tumor take-up rate in the bone at 6 weeks). To confirm that these 28 mice had LuCaP xenograft growth, we measured serum PSA levels. The mouse does not produce PSA, thus this measurement is a specific marker of human CaP tumor in these animals. All 28 mice were positive for PSA (mean \pm SD, 13.2 ± 3.1 ng/ml). The mice with PSA-confirmed tumors were then divided randomly into three groups ($n = 9$ /group; one mouse was not used; serum PSA levels were not statistically different among groups) to be either immediately sacrificed (basal) or receive either sRANK-Fc (200 μ g/mouse) or saline vehicle by i.p. injection three times per week. Mice were sacrificed after 6 weeks of sRANK administration.

The presence of LuCaP tumors for 6 weeks induced an osteosclerotic radiographic response (Fig. 3A, basal *versus* control). After an additional 6 weeks of tumor growth (12 weeks total), the radiographic osteosclerotic appearance increased in the vehicle-treated animals (Fig. 3, vehicle *versus* basal), whereas sRANK-Fc diminished the osteosclerotic appearance (Fig. 3A, sRANK-Fc *versus* vehicle), although it was still increased over that of the basal group. To accurately quantify differences in BMD, we used DEXA (Fig. 3, A and B). The BMD was increased by 15% in the basal group compared with the control group (mice implanted with human fetal bone without tumor). After an additional 6 weeks, the BMD was increased by 12% in the vehicle-treated group compared with the basal group. In contrast, sRANK-Fc limited the increase of BMD to 4% (i.e., ~67% lower increase of BMD then occurred in the vehicle group). These results indicate that LuCaP 35 induces an osteoblastic lesion and that sRANK-Fc inhibits tumor-induced bone formation.

To evaluate the effects of sRANK-Fc at the cellular level of bone, we performed bone histomorphometry on excised implants. The BV:TV, which represents the proportion of total mineralized trabeculae in the total bone in the section, was increased by 19% in the basal group

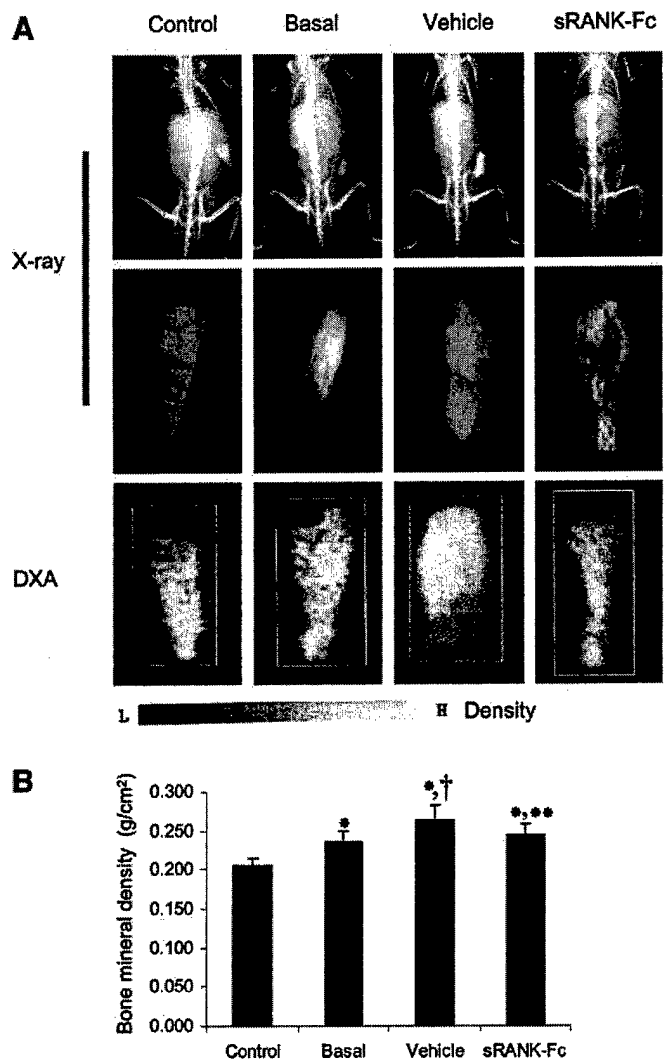


Fig. 3. Radiological examination of LuCaP-induced bone lesions. Implanted human fetal bones in SCID mice were injected with LuCaP 35 single-cell suspension. Six weeks after tumor injection, some mice were sacrificed as the basal group ($n = 9$). The remaining mice were divided to receive either sRANK-Fc (200 μ g/kg) or vehicle (1% BSA in PBS; $n = 9$ /group). Treatments were administered via i.p. injection three times per week for 6 weeks, and the mice were then sacrificed. A, radiograph of LuCaP-induced bone lesions determined by X-ray and DEXA showing osteoblastic lesions with stronger density of the tumor implants compared with the control group (without tumor implantation). Measurement of BMD was performed using DEXA. The color scale indicates low (L) density through high (H) density. B, quantification of BMD for the excised implants in different groups. Values are presented as mean \pm SD. *, $P < 0.01$ compared with control group; †, $P < 0.05$ compared with basal group; **, $P < 0.05$ compared with vehicle-treated group (one-way ANOVA and Fisher's protected least significant difference for *post hoc* analysis).

compared with the control group (Fig. 4A). The BV:TV continued to increase by an additional 11% in the vehicle-treated group compared with the basal group (overall 30% increase in the vehicle group compared with the control group). Administration of sRANK-Fc diminished the increase of BV:TV by 83% (Fig. 4A, sRANK-Fc *versus* vehicle). The osteoblast perimeter (Obs/BS), which represents the number of osteoblasts per millimeter of trabecular bone, was increased by 132% and 152% in the basal and vehicle-treated groups, respectively, compared with the control group (Fig. 4B). Administration of sRANK-Fc did not alter the increase of osteoblast perimeter that occurred in the vehicle-treated group (sRANK-Fc *versus* vehicle). Osteoclast perimeter (Oc/BS), which represents the number of osteoclasts per millimeter of trabecular bone, was increased by ~720% in the basal group *versus* control group (Fig. 4C), indicating that LuCaP

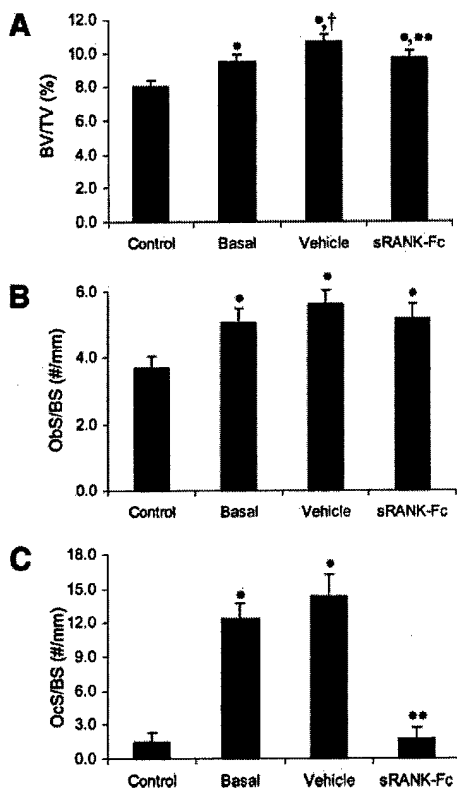


Fig. 4. Effects of sRANK-Fc on bone histomorphometric parameters of LuCaP-induced osteoblastic lesions. Three nonserial sections of each implant were analyzed by using the Bioquant system as described in "Materials and Methods." Five random $\times 200$ magnification fields were evaluated per each section. The values are reported as mean \pm SD ($n = 9$ mice/group). Data were analyzed using one-way ANOVA and Fisher's least significant difference for *post hoc* analysis. *A*, the BV:TV was used to represent total mineralized bone in the trabeculae. *, $P < 0.05$ compared with control; †, $P < 0.01$ compared with basal; **, $P < 0.05$ compared with vehicle-treated group. *B*, the osteoblast perimeter (ObS/BS) represents the number of osteoblasts per millimeter length of bone interface. *, $P < 0.001$ compared with control. *C*, the osteoclast perimeter (OcS/BS) represents the number of osteoclasts per millimeter length of tumor-bone interface. *, $P < 0.001$ compared with control; **, $P < 0.001$ compared with vehicle-treated group.

35 induces osteoclastogenesis. However, it was not further increased in the vehicle-treated mice *versus* basal mice. Administration of sRANK-Fc decreased the osteoclast perimeter to levels similar to the control mice. These results indicate that LuCaP 35 induces both an osteoblastic and osteoclastic responses in bone that can both be inhibited by sRANK-Fc.

To determine whether the tumor-induced changes in bone were reflected systemically in the animals, several bone remodeling markers were measured. Serum human OC, BAP, and urinary Ntx, an indicator of bone resorption, were evaluated. These compounds were not detectable in the control mice (data not shown) although they were detectable in the basal group (Fig. 5). Serum human OC and BAP were decreased by $\sim 30\%$ and 25% , respectively, in the sRANK-Fc-treated mice compared with the vehicle-treated mice (Fig. 5, *A* and *B*). Urinary NTx was reduced by 30% in the sRANK-Fc-treated mice compared with the vehicle-treated mice (Fig. 5C).

To determine the extent of tumor burden, we quantified serum PSA levels in mice. Serum PSA levels, which were undetectable in control mice (data not shown), were increased by $\sim 157\%$ in the vehicle-treated mice compared with the basal mice (Fig. 6A). Administration of sRANK-Fc resulted in only a 50% increase in PSA levels from the levels of basal mice, thus diminishing the increase in that occurred in the vehicle group by $\sim 66\%$ (Fig. 6A). Tumor that stained positive for PSA was readily identified in all of the mice in the various tumor-injected groups (Fig. 6B). Tumor area/total nonmineralized bone area

was increased by 60% in the vehicle-treated group compared with the basal group (represents continued tumor growth; Fig. 6C). In the group receiving sRANK-Fc, the tumor area was increased by 32% compared with the basal group but this was $\sim 50\%$ less than the increase observed in the vehicle-treated group (Fig. 6C). These results showed that sRANK-Fc diminishes LuCaP 35 tumor progression in bone.

To explore whether the ability of sRANK-Fc to inhibit lesions in the bone was a direct effect on tumor cells, we incubated LuCaP 35 cells with sRANK-Fc, then evaluated proliferation rate and cell viability. sRANK-Fc had no effect on these proliferation rates or viability of the LuCaP cells (data not shown). Additionally, we injected LuCaP cells s.c. into the mice, allowed tumors to develop for 6 weeks, then administered sRANK-Fc in a similar fashion as for the studies performed with bone. Administration of sRANK-Fc had no effect on s.c. LuCaP 35 tumor growth rate (Fig. 7). These data suggest that sRANK-Fc does not have a direct inhibitory effect on LuCaP 35.

DISCUSSION

The results from the present study demonstrate that sRANK-Fc diminishes CaP progression in osseous, but not in nonosseous, tissue. Furthermore, the observation that sRANK-Fc did not diminish s.c. growth of the tumor, in combination with the observation that it had no direct effect on the CaP cells *in vitro*, suggests that the ability of sRANK-Fc to inhibit CaP establishment was not because of a direct

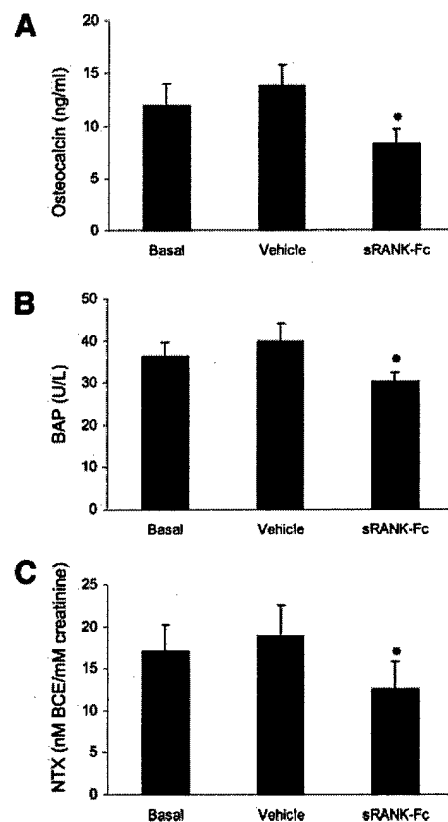


Fig. 5. Effect of sRANK-Fc on systemic bone remodeling markers. Serum and urine were collected from basal, sRANK-Fc, and vehicle treatment groups at the time of their euthanasia. Serum OC, serum BAP, urine NTx, and urine creatinine were measured as described in "Materials and Methods." *A*, serum OC levels. *B*, serum BAP levels. *C*, urine NTx levels are reported as bone collagen equivalents (BCE) normalized to urine creatinine levels. Data are reported as mean \pm SD. Data were analyzed using one-way ANOVA and Fisher's protected least significant difference for *post hoc* analysis. *, $P < 0.01$ compared with vehicle-treated group. Measurements were performed in six to nine individual mice per group.

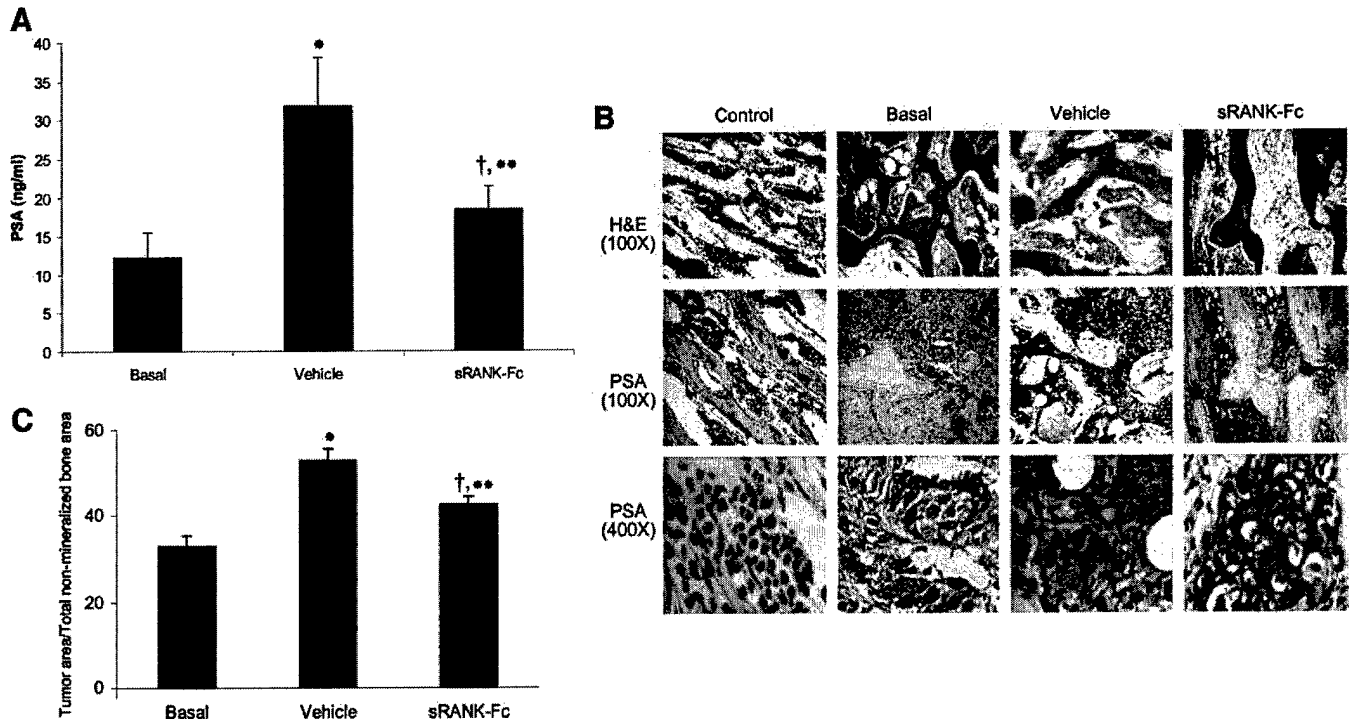


Fig. 6. Effect of sRANK-Fc on LuCaP tumor burden. *A*, serum was collected from basal, sRANK-Fc, and vehicle treatment groups at the time of their euthanasia and subjected to ELISA for PSA. Values are reported as mean \pm SD ($n = 9$ /group). *, $P < 0.001$ compared with basal group; †, $P < 0.01$ compared with basal; **, $P < 0.01$ compared with vehicle-treated group (one-way ANOVA and Fisher's least significant difference for *post hoc* analysis). *B*, histological examination of LuCaP tumors growing in human fetal bone implanted into SCID mice. Formalin-fixed paraffin-embedded sections were stained with H&E or were deparaffinized, rehydrated, and stained for PSA using immunohistochemistry. Brown indicates positive staining of PSA. Representative H&E staining of normal implanted fetal bone without tumor implantation, and implant from mice of basal, vehicle, and sRANK-Fc treatment that paralleled with representative slides of PSA-stained sections were presented. Note in control mice the marrow compartment of human fetal bone implants contain mainly stromal elements and some residual hematopoietic cells, and in tumor implants, the bone marrow contains tumor cells. Specifically, the intramedullary space from the basal and vehicle-treated groups ($\times 100$) has a large component of PSA-positive cells compared with the sRANK-Fc-treated groups. Also, note the increased amount of trabeculae (red) and corresponding decrease in marrow space in the basal and vehicle-treated groups compared with the control or sRANK-Fc-treated groups. *C*, bone tumor burden (total tumor volume as a percentage of noncalcified tissue volume) was determined using bone histomorphometric analysis. Three nonserial sections of each implant were analyzed by using the Bioquant system as described in "Materials and Methods." Five random $\times 200$ magnification fields were evaluated per each section. The values are reported as mean \pm SD ($n = 9$ mice/group). *, $P < 0.001$ compared with basal group; †, $P < 0.01$ compared with basal; **, $P < 0.01$ compared with vehicle-treated group (one-way ANOVA and Fisher's protected least significant difference for *post hoc* analysis).

effect on tumor but rather specific to factors in the bone microenvironment. These data suggest that inhibition of RANKL activity diminishes the progression of CaP skeletal metastasis.

The importance of osteoclastic activity in the development of CaP skeletal metastatic lesions has received little attention because of their overall osteoblastic radiographic appearance. Yet, despite the radiographic appearance, it is clear from histological evidence that CaP metastases form a heterogeneous mixture of osteolytic and osteoblastic lesions (2, 3, 23–25). In fact, histomorphometric analysis of

metastatic lesions reveals that osteoblastic metastases form on trabecular bone at sites of previous osteoclastic resorption, suggesting that bone resorption is required for subsequent osteoblastic bone formation (2). Results from the current study are consistent with previous studies that demonstrate inhibition of RANKL with OPG diminishes CaP establishment or progression of established tumor in bone (7, 26). Taken together, these results support previous published evidence that tumors that metastasize to bone require osteoclastic activity, which releases tumor-supportive growth factors from bone (27, 28). They further extend these studies, because LuCaP is clearly an osteoblastic tumor, as demonstrated by radiographs, DEXA, and bone histomorphometry. Thus, these data clearly demonstrate that osteoclast activity is necessary for the development of osteoblastic CaP tumors.

An active role for osteoclast activity in prostate tumor bone metastasis development is also reflected in clinical data that demonstrate systemic markers of bone resorption are increased in men with CaP skeletal metastases (29, 30) and that bisphosphonates relieve bone pain in this population of patients (31–33). Our observation in the current study that sRANK-Fc reduced several bone systemic bone parameters including OC, BAP, and Ntx in the mice with tumors is consistent with these results. We cannot determine from this study whether the alteration in bone remodeling markers was caused by direct effects of sRANK-Fc on bone or the diminished tumor growth and, thus, decreased tumor impact on bone, or even a combination of these events. Regardless, the presence of tumor was directly associated with increased bone remodeling, suggesting that the tumor has an

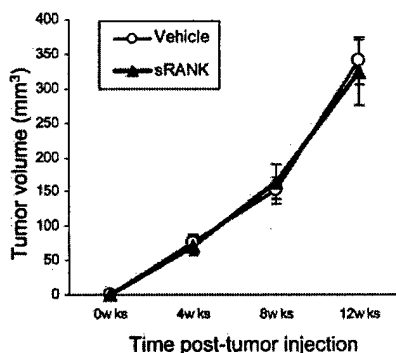


Fig. 7. Effect of sRANK-Fc on s.c. implanted LuCaP tumor growth. LuCaP cells were s.c. injected into SCID mice, and tumors were allowed to develop for 6 weeks, then sRANK-Fc (200 μ g/mouse/day) or vehicle (1% BSA in PBS) were administered via i.p. injection three times per week for 6 weeks, and the mice were then sacrificed. The tumor volume was measured every 4 weeks. The values are reported as mean \pm SD.

impact on bone physiology. This is consistent with our observation that CaP cells including LuCaP (current study), LNCaP, and C4-2B cells express a soluble form of RANKL (7), which can induce osteoclastogenesis.

A major impetus for exploring methods to inhibit RANKL other than OPG is the potential for OPG to act as a survival factor for tumor cells. Specifically, OPG blocked TRAIL-mediated apoptosis of myeloma cells (8) and CaP cells (9). Furthermore, proapoptotic factors such as TNF stimulate OPG secretion from CaP cell lines (34). Taken together, these findings suggest that OPG may function as a survival factor for CaP cells in the bone marrow for microenvironment. Recently, a Phase I clinical trial using either OPG or pamidronate, a bisphosphonate, in patients with either multiple myeloma or breast cancer with radiologically confirmed lytic bone lesions demonstrated comparable inhibition of osteoclast activity, based on NTx levels, between the two compounds (35). However, neither tumor response nor patient survival were evaluated in that study, thus the effect of administering OPG on cancer progression in the cancer patient is unknown at this time. Our observations that sRANK-Fc neither binds TRAIL (data not shown) nor blocks TRAIL-mediated apoptosis of CaP cells suggests that it may be a suitable mediator of RANKL inhibition for clinical use.

The observation that tumor progression was decreased by sRANK-Fc suggests several alternative mechanisms, including the possibility that sRANK-Fc mediates its inhibitory effects either directly on tumor cells or indirectly through its inhibitory effect on RANK and osteoclasts. Similarly, bisphosphonates reduce bone pain in men with CaP skeletal metastases; however, it is unknown whether this effect is caused by inhibiting osteoclastic activity or because of its ability to inhibit tumor cell growth (36–38). In the current study, sRANK-Fc neither inhibited tumor growth or viability *in vitro*, nor did it impact s.c. tumor growth *in vivo*. These observations, taken together with the finding that sRANK-Fc diminished tumor growth in bone, suggests that sRANK-Fc does not have a direct effect on tumor but rather mediates its tumor inhibitory effect indirectly through modulating bone remodeling. However, we cannot rule out that sRANK-Fc has direct inhibitory effect on CaP cells that is dependent on the bone microenvironment.

The observation that sRANK-Fc treatment reduced osteoclast numbers to control levels but only partially diminished indices of tumor-induced osteoblastic activity including BMD and histomorphometric parameters suggests that the tumor cells themselves have bone mineralizing ability that is independent of osteoclastic activity. Thus, because sRANK-Fc only partially reduced tumor volume, the remaining tumor may have promoted osteoblastic activity. This is an agreement with the finding that a CaP cell line injected into mouse bone produced osteoblastic lesions in the presence of low numbers of osteoclasts during the early stages of tumor growth (39). In addition to the pro-osteoblastic activity of tumor remaining after sRANK-Fc treatment, the reduction of osteoclast activity may have resulted in reduction of bone remodeling and, thus, inability of bone resorption to occur to restore the bone to control levels.

In summary, results from the current study demonstrate that an osteoblastic CaP xenograft, LuCaP, produces sRANKL-Fc and induces osteoclastogenesis *in vitro*. Furthermore, this study demonstrated that sRANK-Fc diminishes progression of established LuCaP in bone but not in s.c. tissue, which suggests that osteoblastic tumors require osteoclastic activity to progress and suggests that inhibiting RANKL in men with osteoblastic skeletal metastases will slow tumor progression. Finally, these data suggest that sRANK-Fc is an effective mediator of RANKL inhibition that does not block TRAIL-mediated apoptosis.

ACKNOWLEDGMENTS

We thank Dr. Robert Vessella for providing the LuCaP 35 xenograft.

REFERENCES

- Abrams, H., Spiro, R., and Goldstein, N. Metastases in carcinoma. *Cancer (Phila.)*, 3: 74–85, 1950.
- Charhon, S. A., Chapuy, M. C., Delvin, E. E., Valentin-Opran, A., Edouard, C. M., and Meunier, P. J. Histomorphometric analysis of sclerotic bone metastases from prostatic carcinoma special reference to osteomalacia. *Cancer (Phila.)*, 51: 918–924, 1983.
- Urwin, G. H., Percival, R. C., Harris, S., Beneton, M. N., Williams, J. L., and Kanis, J. A. Generalised increase in bone resorption in carcinoma of the prostate. *Br. J. Urol.*, 57: 721–723, 1985.
- Clarke, N. W., McClure, J., and George, N. J. Disodium pamidronate identifies differential osteoclastic bone resorption in metastatic prostate cancer. *Br. J. Urol.*, 69: 64–70, 1992.
- Clarke, N. The effects of pamidronate disodium treatment in metastatic prostate cancer. *Rev. Contemp. Pharmacother.*, 9: 205–212, 1998.
- Takahashi, N., Udagawa, N., and Suda, T. A new member of tumor necrosis factor ligand family, ODF/OPGL/TRANCE/RANKL, regulates osteoclast differentiation and function. *Biochem. Biophys. Res. Commun.*, 256: 449–455, 1999.
- Zhang, J., Dai, J., Qi, Y., Lin, D. L., Smith, P., Strayhorn, C., Mizokami, A., Fu, Z., Westman, J., and Keller, E. T. Osteoprotegerin inhibits prostate cancer-induced osteoclastogenesis and prevents prostate tumor growth in the bone. *J. Clin. Invest.*, 107: 1235–1244, 2001.
- Shipman, C. M., and Croucher, P. I. Osteoprotegerin is a soluble decoy receptor for tumor necrosis factor-related apoptosis-inducing ligand/Apo2 ligand and can function as a paracrine survival factor for human myeloma cells. *Cancer Res.*, 63: 912–916, 2003.
- Holen, I., Croucher, P. I., Hamdy, F. C., and Eaton, C. L. Osteoprotegerin (OPG) is a survival factor for human prostate cancer cells. *Cancer Res.*, 62: 1619–1623, 2002.
- Yano, Y., Hayashi, Y., Nakaji, M., Nagano, H., Seo, Y., Ninomiya, T., Yoon, S., Wada, A., Hirai, M., Kim, S. R., Yokozaki, H., and Kasuga, M. Different apoptotic regulation of TRAIL-caspase pathway in HBV- and HCV-related hepatocellular carcinoma. *Int. J. Mol. Med.*, 11: 499–504, 2003.
- Smyth, M. J., Takeda, K., Hayakawa, Y., Peschon, J. J., van den Brink, M. R., and Yagita, H. Nature's TRAIL—on a path to cancer immunotherapy. *Immunity*, 18: 1–6, 2003.
- de Bono, J. S., and Rowinsky, E. K. Therapeutics targeting signal transduction for patients with colorectal carcinoma. *Br. Med. Bull.*, 64: 227–254, 2002.
- Oyajobi, B. O., Anderson, D. M., Traianedes, K., Williams, P. J., Yoneda, T., and Mundy, G. R. Therapeutic efficacy of a soluble receptor activator of nuclear factor κ B-IgG Fc fusion protein in suppressing bone resorption and hypercalcemia in a model of humoral hypercalcemia of malignancy. *Cancer Res.*, 61: 2572–2578, 2001.
- Sordillo, E. M., and Pearce, R. N. RANK-Fc: a therapeutic antagonist for RANK-L in myeloma. *Cancer (Phila.)*, 97: 802–812, 2003.
- Childs, L. M., Paschalis, E. P., Xing, L., Dougall, W. C., Anderson, D., Boskey, A. L., Puzas, J. E., Rosier, R. N., O'Keefe, R. J., Boyce, B. F., and Schwarz, E. M. *In vivo* RANK signaling blockade using the receptor activator of NF- κ B:Fc effectively prevents and ameliorates wear debris-induced osteolysis via osteoclast depletion without inhibiting osteogenesis. *J. Bone Miner. Res.*, 17: 192–199, 2002.
- Corey, E., Quinn, J. E., Buhler, K. R., Nelson, P. S., Macoska, J. A., True, L. D., and Vessella, R. L. LuCaP 35: a new model of prostate cancer progression to androgen independence. *Prostate*, 55: 239–246, 2003.
- Corey, E., Quinn, J. E., Bladou, F., Brown, L. G., Roudier, M. P., Brown, J. M., Buhler, K. R., and Vessella, R. L. Establishment and characterization of osseous prostate cancer models: intra-tibial injection of human prostate cancer cells. *Prostate*, 52: 20–33, 2002.
- Nemeth, J. A., Harb, J. F., Barroso, U., Jr., He, Z., Grignon, D. J., and Cher, M. L. Severe combined immunodeficient-hu model of human prostate cancer metastasis to human bone. *Cancer Res.*, 59: 1987–1993, 1999.
- Pearce, R. N., Sordillo, E. M., Yaccoby, S., Wong, B. R., Liau, D. F., Colman, N., Michaeli, J., Epstein, J., and Choi, Y. Multiple myeloma disrupts the TRANCE/osteoprotegerin cytokine axis to trigger bone destruction and promote tumor progression. *Proc. Natl. Acad. Sci. USA*, 98: 11581–11586, 2001.
- Dai, J., Lin, D., Zhang, J., Habib, P., Smith, P., Murtha, J., Fu, Z., Yao, Z., Qi, Y., and Keller, E. T. Chronic alcohol ingestion induces osteoclastogenesis and bone loss through IL-6 in mice. *J. Clin. Invest.*, 106: 887–895, 2000.
- Parfitt, A. M., Drezner, M. K., Glorieux, F. H., Kanis, J. A., Malluche, H., Meunier, P. J., Ott, S. M., and Recker, R. R. Bone histomorphometry: standardization of nomenclature, symbols, and units. Report of the ASBMR Histomorphometry Nomenclature Committee. *J. Bone Miner. Res.*, 2: 595–610, 1987.
- Emery, J. G., McDonnell, P., Burke, M. B., Deen, K. C., Lyn, S., Silverman, C., Dul, E., Appelbaum, E. R., Eichman, C., DiPrinzio, R., Dodds, R. A., James, I. E., Rosenberg, M., Lee, J. C., and Young, P. R. Osteoprotegerin is a receptor for the cytotoxic ligand TRAIL. *J. Biol. Chem.*, 273: 14363–14367, 1998.
- Berruti, A., Piovessan, A., Torta, M., Raucci, C. A., Gorzegno, G., Paccotti, P., Dogliotti, L., and Angeli, A. Biochemical evaluation of bone turnover in cancer patients with bone metastases: relationship with radiograph appearances and disease extension. *Br. J. Cancer*, 73: 1581–1587, 1996.
- Vinholes, J., Coleman, R., and Eastell, R. Effects of bone metastases on bone metabolism: implications for diagnosis, imaging and assessment of response to cancer treatment. *Cancer Treat. Rev.*, 22: 289–331, 1996.

25. Roudier, M., Sherrard, D., True, L., Ott-Ralp, S., Meligro, C., Mberrie, M., Soo, C., Felise, D., Quinn, J. E., and Vessella, R. Heterogenous bone histomorphometric patterns in metastatic prostate cancer. *J. Bone Miner. Res.*, **15S1**: S567, 2000.
26. Yonou, H., Kanomata, N., Goya, M., Kamijo, T., Yokose, T., Hasebe, T., Nagai, K., Hatano, T., Ogawa, Y., and Ochiai, A. Osteoprotegerin/osteoclastogenesis inhibitory factor decreases human prostate cancer burden in human adult bone implanted into nonobese diabetic/severe combined immunodeficient mice. *Cancer Res.*, **63**: 2096–2102, 2003.
27. Guise, T. A. Molecular mechanisms of osteolytic bone metastases. *Cancer (Phila.)*, **88**: 2892–2898, 2000.
28. Clarke, N. W., McClure, J., and George, N. J. Morphometric evidence for bone resorption and replacement in prostate cancer. *Br. J. Urol.*, **68**: 74–80, 1991.
29. Garnero, P., Buchs, N., Zekri, J., Rizzoli, R., Coleman, R. E., and Delmas, P. D. Markers of bone turnover for the management of patients with bone metastases from prostate cancer. *Br. J. Cancer*, **82**: 858–864, 2000.
30. Fontana, A., and Delmas, P. D. Markers of bone turnover in bone metastases. *Cancer (Phila.)*, **88**: 2952–2960, 2000.
31. Dawson, N. A. Therapeutic benefit of bisphosphonates in the management of prostate cancer-related bone disease. *Expert Opin. Pharmacother.*, **4**: 705–716, 2003.
32. Pelger, R. C., Hamdy, N. A., Zwiderman, A. H., Lycklama a Nijeholt, A. A., and Papapoulos, S. E. Effects of the bisphosphonate olpadronate in patients with carcinoma of the prostate metastatic to the skeleton. *Bone*, **22**: 403–408, 1998.
33. Heidenreich, A., Hofmann, R., and Engelmann, U. H. The use of bisphosphonate for the palliative treatment of painful bone metastasis due to hormone refractory prostate cancer [In Process Citation]. *J. Urol.*, **165**: 136–140, 2001.
34. Penno, H., Silfversward, C. J., Frost, A., Brandstrom, H., Nilsson, O., and Ljunggren, O. Osteoprotegerin secretion from prostate cancer is stimulated by cytokines, in vitro. *Biochem. Biophys. Res. Commun.*, **293**: 451–455, 2002.
35. Body, J. J., Greipp, P., Coleman, R. E., Facon, T., Geurs, F., Femand, J. P., Harousseau, J. L., Lipton, A., Mariette, X., Williams, C. D., Nakanishi, A., Holloway, D., Martin, S. W., Dunstan, C. R., and Bekker, P. J. A phase I study of AMG-007, a recombinant osteoprotegerin construct, in patients with multiple myeloma or breast carcinoma related bone metastases. *Cancer (Phila.)*, **97**: 887–892, 2003.
36. Corey, E., Brown, L. G., Quinn, J. E., Poot, M., Roudier, M. P., Higano, C. S., and Vessella, R. L. Zoledronic acid exhibits inhibitory effects on osteoblastic and osteolytic metastases of prostate cancer. *Clin. Cancer Res.*, **9**: 295–306, 2003.
37. Coleman, R. E. Optimising treatment of bone metastases by Aredia™ and Zometa™. *Breast Cancer*, **7**: 361–369, 2000.
38. Boissier, S., Ferreras, M., Peyruchaud, O., Magnetto, S., Ebetino, F. H., Colombel, M., Delmas, P., Delaisse, J. M., and Clezardin, P. Bisphosphonates inhibit breast and prostate carcinoma cell invasion, an early event in the formation of bone metastases. *Cancer Res.*, **60**: 2949–2954, 2000.
39. Lee, Y., Schwarz, E., Davies, M., Jo, M., Gates, J., Wu, J., Zhang, X., and Lieberman, J. R. Differences in the cytokine profiles associated with prostate cancer cell induced osteoblastic and osteolytic lesions in bone. *J. Orthop. Res.*, **21**: 62–72, 2003.

Author Proof

In Vivo Real-Time Imaging of TGF- β -Induced Transcriptional Activation of the RANK Ligand Gene Promoter in Intraosseous Prostate Cancer

Jian Zhang,¹ Yi Lu,² Jinlu Dai,¹ Zhi Yao,² Riko Kitazawa,³ Sohei Kitazawa,³ Xinping Zhao,⁴ Daniel E. Hall,⁵ Kenneth J. Pienta,⁶ and Evan T. Keller^{1*}

¹Department of Pathology and Unit for Laboratory Animal Medicine, School of Medicine, University of Michigan, Ann Arbor, Michigan

²Department of Immunology, Tianjin Medical University, Tianjin, China

³Division of Molecular Pathology, Kobe University, Kobe, Japan

⁴Department of Neurology, School of Medicine, University of Michigan, Ann Arbor, Michigan

⁵Center for Molecular Imaging, School of Medicine, University of Michigan, Ann Arbor, Michigan

⁶Department of Medicine and Urology, School of Medicine, University of Michigan, Ann Arbor, Michigan

BACKGROUND. Current animal models of prostate cancer (CaP) bone metastasis do not allow measurement of either tumor growth in bone over time or activation of gene promoters in intraosseous tumors. To develop these methods, we used bioluminescent imaging (BLI) to determine if expression of receptor activator of NF- κ B ligand (RANKL), a pro-osteoclastogenic factor that promotes CaP bone metastases, is modulated by the bone matrix protein transforming growth factor- β (TGF- β) in vivo.

METHODS. C4-2B human CaP cells were treated with TGF- β in vitro and RANKL mRNA and protein production were measured by polymerase chain reaction (PCR) and ELISA, respectively. Then C4-2B cells stably transfected with the RANKL promoter driving luciferase (lux) were injected intra-tibially into severe combined immunodeficient (SCID) mice. Tumors were subjected to BLI every 2 weeks for 6 weeks and serum prostate specific antigen (PSA) was measured using ELISA. Vehicle (V), 1,25 dihydroxyvitamin D (VitD), or TGF- β was administered to mice with established tumors and BLI to measure RANKL promoter activity was performed. Tumors were then subjected to immunohistochemistry for lux and assayed for RANKL mRNA levels.

RESULTS. TGF- β induced RANKL protein and mRNA expression and activated the RANKL promoter activity in a dose-dependent manner in vitro. BLI demonstrated an increase in intraosseous tumor size over time, which correlated with serum PSA levels. Administration of TGF- β and VitD to mice with established intraosseous tumors increased lux activity compared

Abbreviations: ANOVA, analysis of variance; BLI, bioluminescent imaging; CaP, prostate cancer; DMEM, Dulbecco's minimum essential medium; ECM, extracellular matrix; FBS, fetal bovine serum; GAPDH, glyceraldehyde-3-phosphate dehydrogenase; HRP, horseradish peroxidase; OPG, osteoprotegerin; PAGE, polyacrylamide gel electrophoresis; PBS, phosphate-buffered saline; PCR, polymerase chain reaction; PMSF, phenylmethylsulfonyl fluoride; PSA, prostate-specific antigen; PTH, parathyroid hormone; PTHrP, parathyroid hormone-related protein; RANK, receptor activator of NF- κ B; RANKL, receptor activator of NF- κ B ligand; RT-PCR, reverse transcription-polymerase chain reaction; SCID, severe combined immunodeficient; SDS, sodium dodecyl sulfate; TGF- β , transforming growth factor- β ; TNF, tumor necrosis factor; VitD, 1,25-dihydroxyvitamin D.

Grant sponsor: USAMRMC Prostate Cancer Research Program; Grant number: DAMD17-03-1-0092; Grant sponsor: National Cancer Institute; Grant number: SPORE 1 P50 CA69568; Grant sponsor: University of Michigan's Cancer Center; Grant number: 5 P30 CA46592.

*Correspondence to: Evan T. Keller, DVM, PhD, Unit for Laboratory Animal Medicine, and Department of Pathology, University of Michigan School of Medicine, 1500 E. Medical Ctr. Dr., Ann Arbor, MI 48109-0940. E-mail: etkeller@umich.edu

Received XXXXXX^{Q1}; Accepted XXXXXX

DOI 10.1002/pros.00000

Published online 00 Month 2003 in Wiley InterScience (www.interscience.wiley.com).

to V. Intratibial tumor RANKL mRNA expression paralleled the increased promoter activity. Immunohistochemistry confirmed the presence of lux in the intraosseous tumors.

CONCLUSIONS. These results demonstrate the ability to measure intraosseous tumor growth over time and gene promoter activation in an established intraosseous tumor in vivo and also demonstrate that TGF- β induces activates the RANKL promoter. These results provide a novel method to explore the biology of CaP bone metastases. *Prostate* 9999: 1–11, 2004.

© 2004 Wiley-Liss, Inc.

KEY WORDS: TGF- β ; RANKL transcription; bioluminescent imaging; prostate cancer; bone metastasis

INTRODUCTION

Prostate cancer (CaP) has a great predisposition to metastasizing to bone where it forms mixture of osteolytic and osteoblastic lesions (reviewed in Refs. 1,2). The importance of the osteolytic component to the development of CaP bone metastases has been demonstrated by both histological examination of clinical metastases and several in vivo studies [3–6]. CaP-induced bone resorption is primarily caused by osteoclasts [7]. Receptor activator of NF- κ B ligand (RANKL), a tumor necrosis factor (TNF) family member, plays an essential role for induction of osteoclastogenesis through binding and activating RANK on osteoclast precursors [8]. Osteoprotegerin (OPG) is a soluble decoy receptor for RANKL and blocks the binding of RANKL to RANK resulting in inhibition of osteoclastogenesis [9]. RANKL expression is increased in CaP cells at bone metastatic sites of CaP patients [10] and in some but not all CaP cell lines [5,11]. In addition, CaP-induced osteoclast activity is mediated through RANKL and can be inhibited by administration of OPG [5,6]. Thus, understanding the regulation of RANKL in CaP cells may help design therapies to inhibit CaP bone metastases.

RANKL is expressed in a variety of cells including bone-derived endothelial cells, human umbilical vein endothelial cells, T lymphocytes, osteoblasts, and bone marrow stromal cells [12]. However, there are limited published data regarding the regulation of RANKL expression. It has been reported that activation of T cells [13,14], parathyroid hormone [15,16], 1,25-dihydroxyvitamin D (VitD) [17], and inflammatory cytokines [18,19] upregulate RANKL expression and that vitamin K downregulates RANKL expression [20]. However, the mechanism of how RANKL expression is regulated by these factors has not been reported.

The bone extracellular matrix (ECM) is rich in a variety of growth factors that may influence RANKL expression. For example, transforming growth factor- β (TGF- β), which is abundantly stored in bone ECM, promotes osteoclastogenesis [21]. TGF- β is released from the bone ECM during cancer-induced bone resorption [22]. Although TGF- β is released during bone

resorption and may influence CaP progression in bone, its ability to modulate RANKL expression in CaP cells is currently unknown.

Evaluating regulation of gene expression at the gene promoter level is typically done in vitro with promoter-driven reporter assays or nuclear run on assays. These assays are typically insensitive and complicated, respectively, and do not necessarily reflect regulation of the gene in the endogenous environment. Due to these limitations, improved methods to identify gene promoter activation in vivo would enhance investigators' ability to explore gene regulation. In this study, we tested if TGF- β induces RANKL expression at the promoter level in established intraosseous CaP tumors in vivo using a novel method to identify activation of the promoter in vivo.

MATERIALS AND METHODS

Reagents

For in vitro experiments, 1,25-dihydroxyvitamin D3 (VitD3) Sigma-Aldrich, Inc., (St. Louis, MO) was diluted to 10^{-3} M stock solution in ethanol, then diluted further in phosphate-buffered saline (PBS) as required. For in vivo experiments, VitD3 was diluted in propylene glycol. TGF- β (R&D Systems, Minneapolis, MN) was diluted as required into PBS.

Animals

Six-week-old male severe combined immunodeficient (SCID) mice (Charles River, Wilmington, MA) were housed under pathogen-free conditions. An animal protocol for this study was approved by the University of Michigan Animal Care and Use Committee.

Cells

The human prostate C4-2B cells (UroCor, Inc., Oklahoma City, OK) are derived from LNCaP cells through several passages via castrated nude mice and isolated from the tumor that metastasize to bone [23]. The C4-2B cells were maintained in T medium (80% Dulbecco's minimum essential medium (DMEM,

Life Technologies, Inc., Grand Island, NY), 20% F12K (Irving Scientific, Santa Ana, CA), 3 g/L NaHCO₃, 100 U/L penicillin G, 100 µg/ml streptomycin, 5 µg/ml insulin, 13.6 pg/ml triiodothyronine, 5 µg/ml apo-transferrin, 0.25 µg/ml biotin, 25 µg/ml adenine) that was supplemented with 10% fetal bovine serum (FBS). DU-145 and PC-3 CaP cells (American Type Culture Collection, Manassas, VA) were maintained in RPMI media supplemented with 10% FBS.

RANKL Promoter Cloning

A total of 1×10^6 recombinants from the human genomic library (Clontech) were screened by plaque hybridization using a probe consisting of polymerase chain reaction (PCR)-amplified exon 1 of the human RANKL gene as previously published [24]. A 1,974 bp clone (Genbank AF544022) was isolated. Primer extension using a poly(T) + oligo positioned the major transcriptional initiation site 157 nucleotides upstream from the initial methionine site, and this was assigned the +1 position. The 5'-flanking sequence around the transcription initiation site of the human RANKL gene contained TATA- and CAAT-boxes at -22 and -56 bp.

Sac I and Hind III adaptors were ligated onto the 5'- and 3'-ends, respectively, of the promoter. The pGL3-Basic vector (Promega, Madison, WI) was digested with Sac I and Hind III and the modified promoter fragment was directionally ligated into the plasmid upstream of the luciferase (lux) coding sequence. Both strands were sequenced by the dideoxy nucleotide termination method with an ABI PRISM 310 automated sequence analyzer (Applied Biosystems) to confirm the cloning process.

Stable Transfection

C4-2B (5×10^5) cells plated in 60 mm dishes then were stably co-transfected with RANKL promoter driving lux plasmid (1 µg) or empty PGL-3-basic vector as control (1 µg) with an expression vector for neomycin resistance (pcDNA3.1+) (0.1 µg) with the use of SuperFect reagent (Qiagen, Valencia, CA) according to the manufacturer's instructions. Selection for the neomycin resistance was initiated 48 hr after transfection by adding 600 µg/ml of G418 (Life Technologies, Inc.) to the culture medium. The selection medium was changed every 4 days for 5 weeks. Surviving G418-resistant cells were pooled and tested for lux expression. Lux expression was stably maintained after ten passages in the absence of G418.

Tumor Cell Inoculation

For intratibial injection tumors, single-cell suspensions (3×10^5 cells) of C4-2B cells in T media were injected into the right tibia of the male SCID mice

($n = 8$ per group) as described previously [5]. Briefly, mice were anesthetized (135 mg ketamine, 15 mg xylazine/kg body weight), the knee was flexed, and a 26 g, 3/8-inch needle was inserted into the proximal end of right tibia followed by injection of 20 µl of the cell suspension.

For subcutaneous tumor development, C4-2B cells were resuspended in T-media plus 10% FBS and cells (1×10^6) were then injected in the flank at 100 µl/site using a 23 G needle. Subcutaneous tumor growth was identified by palpation and two perpendicular axes were measured and the tumor volume was calculated using the formula: volume = length \times width²/2, as previously described [5].

Radiographic Analysis

Magnified flat radiographs were taken with a Faxitron (Faxitron X-Ray Corp., Wheeling, IL).

Luciferase Measurement

In some instances, as indicated in the figure legends, *in vitro* lux production was measured using a luminometer (Lumat LB9501, Berthold). In other instances, *in vitro* and *in vivo* bioluminescence imaging were performed on a cryogenically cooled imaging system (Xenogen Corporation, Alameda, CA) coupled to a data acquisition computer. The stable transfectant used in *in vivo* study was first tested *in vitro* by adding 20-µl luciferin (40 mg/ml) into the 96-wells plate. Luminescence emitted from the plate was integrated for 1 min starting immediately after adding luciferin. For the *in vivo* study, prior to imaging, animals were anesthetized in an acrylic chamber with 1.5% isofluorane/air mixture and injected through intraperitoneal with 40 mg/ml of luciferin potassium salt in PBS at a dose of 150 mg/kg body weight as previously described [25]. A digital gray scale animal image was acquired followed by acquisition and overlay of a pseudocolor image representing the spatial distribution of detected photon counts emerging from active lux within the animal. Photon counts emitted from the mouse were collected for 1 min starting 10 min after injection of luciferin. Images were processed and photon counts were quantified using Living Image software (Xenogen Corporation).

Histopathology and Immunohistochemistry

Histopathology was performed as we have previously described [5]. Briefly, bone specimens were fixed in 10% formalin for 24 hr, then decalcified using 12% EDTA for 72 hr. The specimens were then paraffin embedded, sectioned (5 µM) and stained with hematoxylin and eosin (H&E) to assess histology.

Non-stained tissues sections were deparaffinized and rehydrated then stained for lux with mouse anti-lux monoclonal antibody (Sigma) and biotinylated anti-mouse IgG antibody for detection using peroxidase staining as recommended by the manufacturer (mouse ABC Staining Systems; Santa Cruz Biotechnology, Santa Cruz, CA).

Western Blot Analysis

To evaluate the effect of TGF- β on RANKL protein expression in C4-2B cells (2×10^6) were plated in T75 flasks and treated with different dose of TGF- β , vehicle (V), or VitD for 24 hr and the cells washed twice with PBS and then lysed in RIPA buffer ($1 \times$ PBS, 1% Nonidet P-40, 0.5% sodium deoxycholate, 0.1% sodium dodecyl sulfate (SDS)) with 100 ng/ml PMSF. proteins (40 μ g/lane) from the cell lysates were applied to SDS-polyacrylamide gel electrophoresis (PAGE) followed by Western blot analysis with mouse anti-human RANKL monoclonal antibody (R&D Systems). The antibody binding was revealed using a horseradish peroxidase (HRP)-conjugated anti-mouse IgG (Amersham Pharmacia Biotech, Piscataway, NJ) and enhanced chemiluminescence (ECL) blot detection system (Amersham Pharmacia Biotech).

Real-Time PCR

To isolate total mRNA from tumors within the mouse tibia, individual tibiae were excised from the mice and the distal 1 cm of the tibia was isolated using bone cutters, then ground using a steel bone mill (BioComp MiniMill, Biomedical Composites, Ltd., Ventura, CA) in 1 ml of RNase-free PBS. The ground substance was vortexed for 1 min, the chips allowed to settle and the supernatant was aspirated and the pellet was mixed with 1 ml of Trizol reagent (Life Technologies, Inc.), vortexed for 30 sec, then homogenized for three 10 sec intervals and centrifuged at 10,000 rpm for 30 sec. The supernatant is collected and subjected to total RNA isolation as described by the manufacturer. To isolate total mRNA from C4-2B cells in vitro, Trizol Reagent (Life Sciences) was added to the plates as described by the manufacturer. Total RNA (200 ng) was subjected to real-time reverse transcription-PCR (RT-PCR) using a LightCycler SYBR Green I RNA amplification kit according to the manufacturer's instructions (Roche Diagnostics, Indianapolis, IN). RT-PCR reactions were subjected to 45 cycles of 94°C for 5 sec, 55°C for 10 sec, and 72°C for 1 min. RT-PCR of glyceraldehyde-3-phosphate dehydrogenase (GAPDH) transcripts was used as an internal control to normalize for loading differences between samples. PCR primers used for detection of RANKL mRNA consisted of upstream: 5'-GCTTGAAGCTCAGCCTTTTGCTCAT-3'

and downstream: 5'-GGGGTTGGAGACCTCGATGCTGATT-3'. PCR primers used for detection of GAPDH mRNA consisted of upstream: 5'-GGAGTCAACG-GATTTGGT-3' and downstream: 5'-GTGATGGGAT-TTCCATTGAT-3'.

Prostate Specific Antigen (PSA) Measurement

Blood was collected via tail vein every 2 weeks during the study and serum was harvested and frozen at -80°C until assayed. Total PSA levels in serum were determined using the Accucyte Human PSA assay (Cytimmune Sciences, Inc., College Park, MA). The sensitivity of this assay is 0.488 ng/ml.

Statistical Analysis

Statistical analysis of the data was performed using Statview Software (Abacus Concepts, Berkeley, CA). Analysis of variance (ANOVA) was used for initial analysis followed by Fisher's protected least significance for post-hoc analyses. Differences were considered to be significantly significant when a *P*-value <0.05 was found. To compare the relation between PSA and tumor volume, simple linear regression was used.

RESULTS

To determine if TGF- β induces RANKL expression in C4-2B CaP cells in vitro. C4-2B cells were incubated with increasing doses of TGF- β then RANKL protein in the culture media and cellular RANKL mRNA expression was measured. Additionally, VitD, a known inducer of RANKL expression [26], was used as a positive control. TGF- β induced RANKL protein expression in dose-responsive fashion with approximately a fourfold induction at 10 ng/ml of TGF- β (Fig. 1). Similarly, TGF- β induced RANKL mRNA expression in dose-responsive fashion with approximately a sevenfold induction at 10 ng/ml of TGF- β (Fig. 1). These data indicate that TGF- β can induce RANKL protein through increasing RANKL mRNA steady state levels. Increased steady state levels may be due to either increased transcriptional activation and/or decreased mRNA degradation. To determine if activation of the RANKL promoter could contribute to the increased RANKL mRNA expression, we stably transfected C4-2B cells with a lux reporter vector driven by the human RANKL promoter then treated the stably transfected cells with TGF- β . RANKL promoter activity, as indicated by lux levels, was then measured using luminescent imaging. TGF- β induced RANKL in a dose-responsive fashion with approximately a 3.7-fold induction at 10 ng/ml of TGF- β (Fig. 2). VitD also induced the RANKL promoter as expected. Taken together, these data demonstrate that TGF- β increases

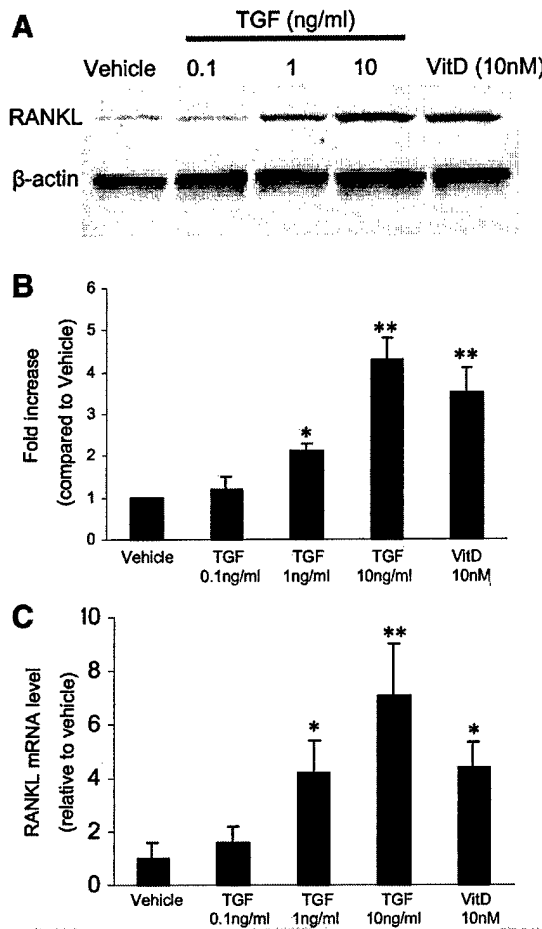


Fig. 1. Transforming growth factor- β (TGF- β) induces RANKL protein and mRNA expression in C4-2B cells. **A:** C4-2B cells were treated with vehicle (V), TGF- β , or 1,25-dihydroxyvitamin D (VitD3) for 24 hr at the indicated doses. Total cellular protein from C4-2B cells was subjected to Western blot analysis for RANKL. Then the membrane was stripped and reprobed for β -actin. **B:** RANKL protein band density was quantified using densitometric analysis. RANKL bands were normalized to β -actin bands. Results are reported as mean \pm SD from three independent experiments. * $P < 0.01$, ** $P < 0.001$ as compared with vehicle-treated cells. **C:** Total RNA was isolated from C4-2B cells treated as indicated. RANKL mRNA expression was evaluated by real-time PCR. Human glyceraldehyde-3-phosphate dehydrogenase (GAPDH) mRNA was used to normalize between samples. Results are reported as mean \pm SD from three independent experiments, each one performed with triplicates measurements of PCR products. * $P < 0.01$, ** $P < 0.001$ as compared with vehicle treated cells.

RANKL expression, in part, through activation of the RANKL promoter.

To better recapitulate the RANKL promoter response in CaP bone metastases, the response of the RANKL promoter to TGF- β in vivo in C4-2B CaP tumors established in bone was evaluated. Accordingly, we injected C4-2B cells stably-transfected with

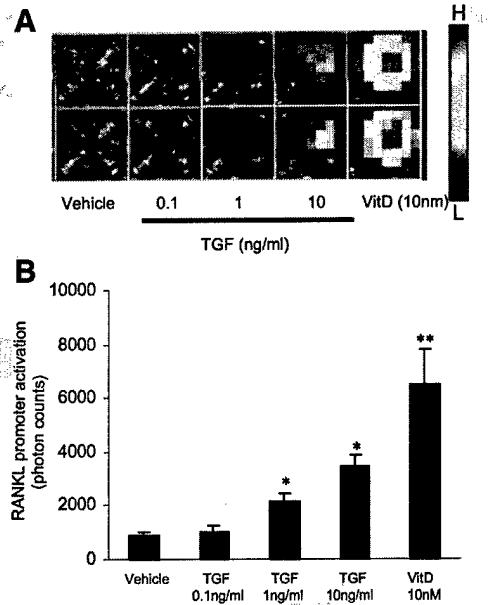


Fig. 2. TGF- β induces RANKL transcription in C4-2B cells in vitro. **A:** C4-2B cells were stably transfected with human RANKL promoter (1.97 kb) driving luciferase (lux). The stably transfected C4-2B clones were pooled and plated in 96-well-plates and treated with vehicle (V), TGF- β , or 1,25-dihydroxyvitamin D (VitD3) for 24 hr at indicated doses. Luciferin was added to each well and imaging was performed using IVISTM Xenogen Imaging system (Xenogen Corporation, Alameda, CA). Photon counts were collected over a minute period. A duplicate sample is shown. The scale bar indicates luminescence intensity from high (H) to low (L). **B:** Photon counts were quantified. Results are reported as the mean \pm SD from duplicates measurements of pooled clones. * $P < 0.01$, ** $P < 0.001$ compared with vehicle.

the RANKL-lux reporter vector into the tibia of mice and tumor was allowed to grow over 6 weeks. To identify development of tumors, radiographs of the tibia were taken every 2 weeks after tumor injection up to 6 weeks. Radiographic changes were not identified until 6 weeks after tumor injection (Fig. 3A). They consisted of mixed osteolytic and osteoblastic changes as previously reported for C4-2B cells in bone. In contrast, tumor was identifiable as early as 2 weeks using bioluminescent imaging (BLI) and increasing tumor growth in bone was detectable over time using BLI of living mice (Fig. 3B,C). To ensure that the increased BLI reflected tumor burden, serum PSA was measured. The mouse does not make PSA, thus the serum PSA confirms the C4-2B tumor burden in the mice. PSA levels increased over time in a similar fashion to the lux levels (Fig. 3D). The BLI of the tumors was strongly correlated with PSA levels (Fig. 3E). These data indicate that BLI can be used to non-invasively measure tumor growth in bone over time in mice.

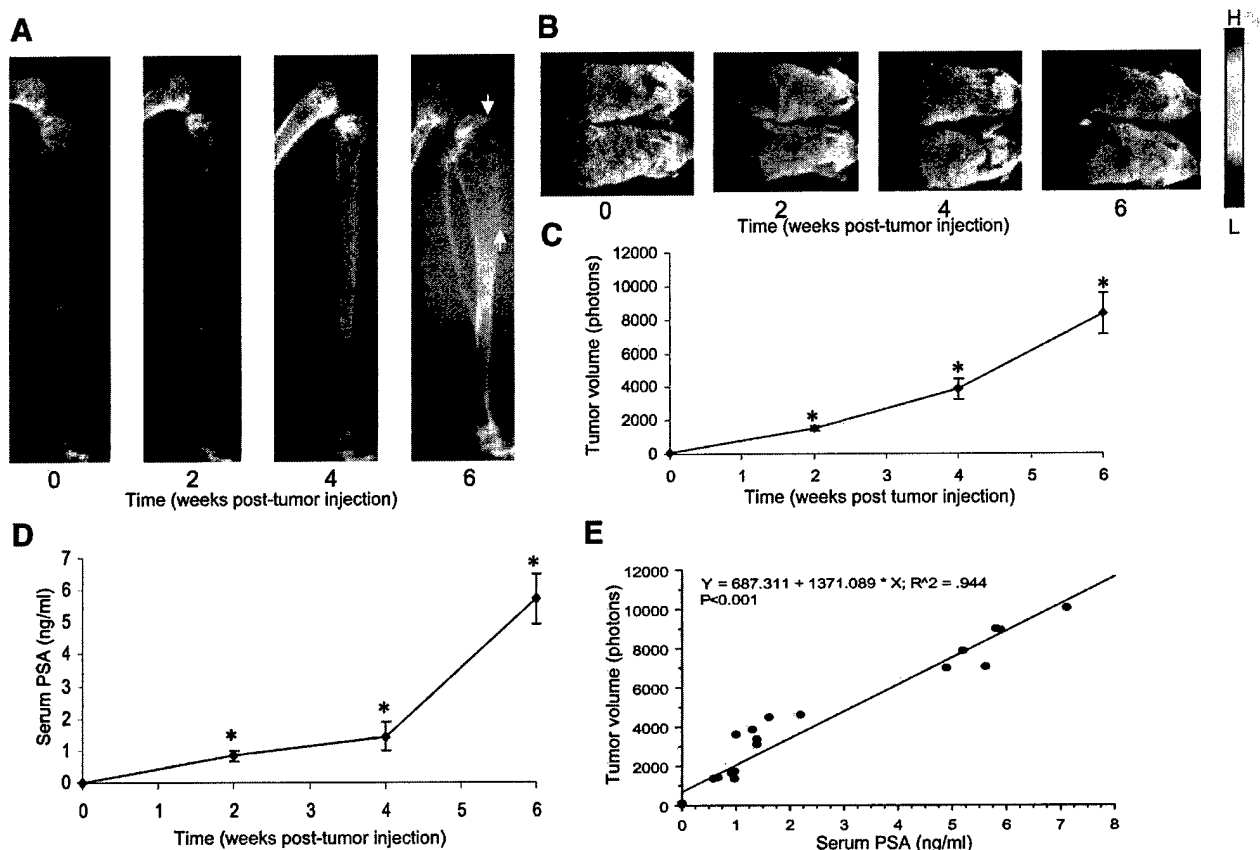


Fig. 3. Bioluminescent imaging (BLI) can be used to detect tumor growth in bone in vivo over time. C4-2B prostate cancer (CaP) cells were stably transfected with a reporter vector of the RANKL promoter driving lux. The transfected C4-2B cells were injected intratibially into severe combined immunodeficient (SCID) mice ($n = 6$). Mice were subjected to radiographs and BLI for lux every 2 weeks post-tumor injection at which time serum was collected and frozen for prostate specific antigen (PSA) evaluation. **A:** Radiographs of a mouse tibia injected with C4-2B CaP cells. Tumor-induced changes are noted between the arrowheads. **B:** Representative scan of two mice demonstrating luminescence in the tibia. Lower mouse is the same as in (A). The scale bar indicates luminescence intensity from high (H) to low (L). **C:** Quantification of luminescence from six animals. Photon counts were collected over a minute period. Results are reported as the mean \pm SD. * $P < 0.01$ compared to the measurement 2 weeks prior. **D:** Serum PSA levels were determined using ELISA. Results are reported as the mean \pm SD. * $P < 0.01$ compared to the measurement 2 weeks prior. **E:** Regression analysis between BLI-measured tumor volume and serum PSA.

Fig. 4. BLI detects that TGF- β activates the RANKL promoter in C4-2B cells in bone in vivo. C4-2B CaP cells were stably transfected with a reporter vector of the RANKL promoter driving lux. The transfected C4-2B cells were injected intratibially into SCID mice tumors were allowed to develop over 6 weeks and vehicle (phosphate-buffered saline, PBS), TGF- β (100 ng/mouse), or 1,25-dihydroxyvitamin D (VitD3) (200 ng/mouse) in propylene glycol was then administered intraperitoneally into the mice ($n = 6$ /group). The mice were then anesthetized at the indicated times pre- or post-injection and BLI was performed. Photon counts were collected over a minute period. **A:** Representative BLI images of mice treated with either TGF- β or VitD3. The same mouse is shown over time for each treatment. The scale bar indicates luminescence intensity from high (H) to low (L). **B:** Luciferin was injected 10 min prior to the desired timepoint for BLI measurement. Luminescence emitted from the mouse was then integrated for 1 min starting 10 min after injection of luciferin. Results are reported as mean \pm SD ($n = 6$ /group). * $P < 0.05$, ** $P < 0.01$ compared with pre-treatment (pre-) for that compound. **C:** Stably transfected C4-2B clones were pooled and plated in 12-well-plates and treated with TGF- β (10 ng/ml) or 1,25-dihydroxyvitamin D (VitD3; 10 nM) for 24 hr. Cells were then collected for measurement of lux on a luminometer. Results are reported as mean \pm SD of two experiments. * $P < 0.05$, ** $P < 0.01$ compared with pre-treatment (pre-) for that compound. **D:** A section of the intratibial tumors were mechanically ground and then homogenized to collect total RNA which was then subjected to real-time PCR for RANKL mRNA and GAPDH mRNA. RANKL mRNA levels were normalized to GAPDH mRNA levels. Results are reported as mean \pm SD. * $P < 0.01$ compared with vehicle. **E:** Sections of intratibial tumors were decalcified and processed for histology. Sections were stained with hematoxylin and eosin (H&E) or subjected to immunohistochemistry for lux. The top sections are 100 \times magnification and the bottom sections (indicated by the squares in the top section) are 400 \times magnification. The bar represents the cartilage epiphysis. Bone is represented by pink osteoid. Tumor cells are seen surrounded by bone and are indicated by the arrow. In the lux sections, lux is represented by the brown color.

Once tumors were developed, VitD (as positive control) and TGF- β were administered to the mice. Both VitD and TGF- β transiently induced RANKL promoter activity in the C4-2B cells in bone (Fig. 4A,B). To determine if the observed pattern of RANKL promoter activity in vivo was due to pharmacokinetics of VitD or TGF- β , we exposed cells in vitro to these compounds and measured lux expression. The tran-

sient nature of the RANKL promoter induction was repeated in vitro (Fig. 4C) indicating this was not a pharmacokinetic effect. To confirm that VitD and TGF- β -induced promoter activity was associated with increased RANKL production in vivo, we measured RANKL mRNA levels in the bone tumors. Both VitD and TGF- β induced RANKL mRNA expression (Fig. 4D). Histology of the tumors was performed and

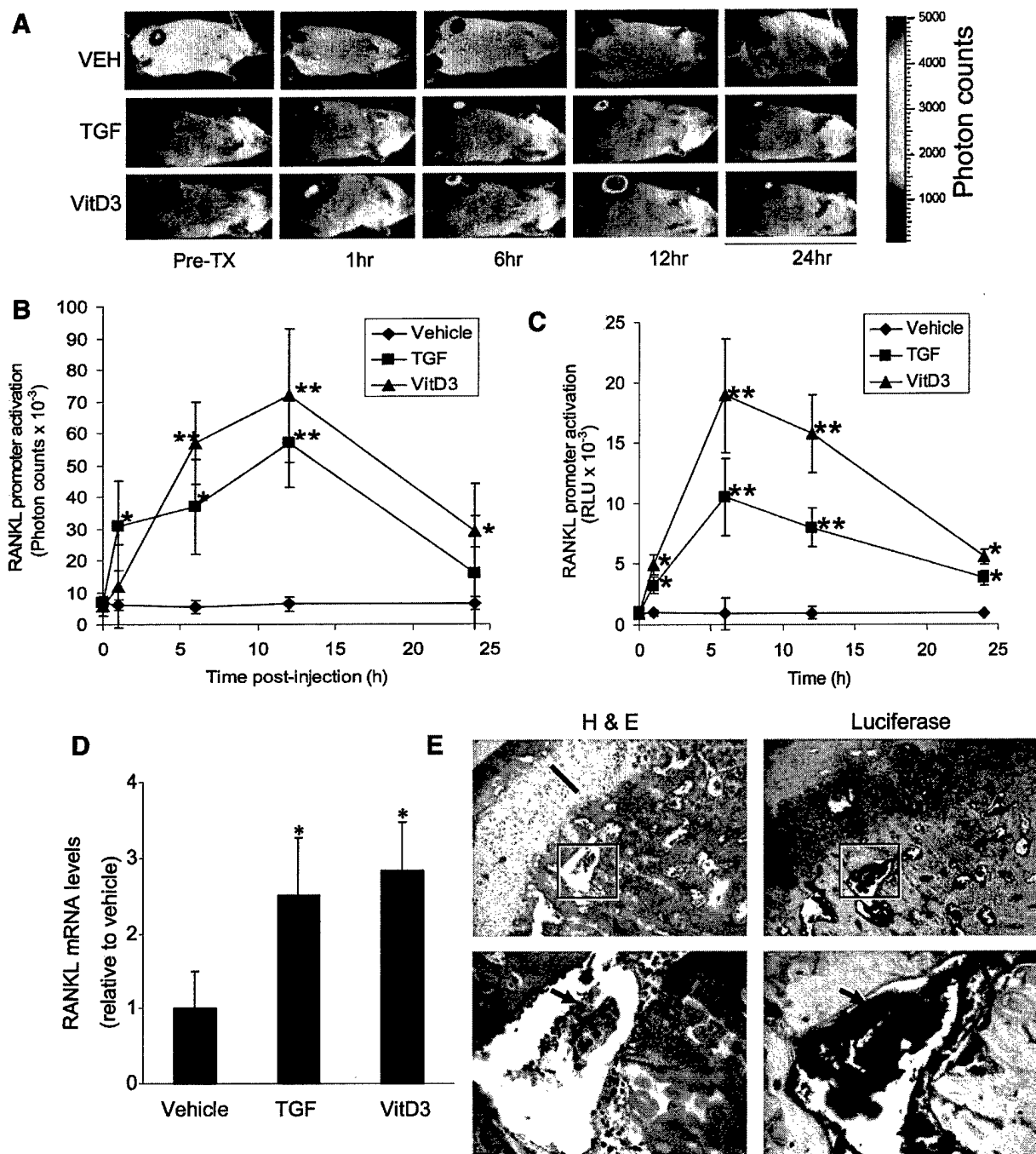


Fig. 4.

confirmed the presence of tumor in bone (Fig. 4E). Furthermore, to confirm that the tumors were making lux, we performed immunohistochemistry for lux on the tumor sections. Lux was colocalized within the tumor cells in bone (Fig. 4E), which confirms that the C4-2B cells were expressing lux in the tumor site and that the RANKL promoter was active at this site. Taken together, these results demonstrate that TGF- β induces the RANKL promoter in bone and that BLI imaging can be utilized to measure promoter activation within tumors in vivo.

DISCUSSION

In the current study, we demonstrated both the ability to quantify activation of a gene promoter in intraosseous CaP as well as quantify intraosseous CaP tumor growth over time. In addition to these methodological advances, we identified that TGF- β , a protein found at high levels in the bone ECM, promotes CaP-mediated RANKL production through activation, in part, of the RANKL promoter. Taken together, these results contribute to both the understanding of how bone crosstalks with CaP, as well as providing new methodologies to explore bone and CaP crosstalk.

Evaluating promoter activity in vitro is fraught with inconsistencies. For example, the substrate of the cell culture plates can influence signaling in the cells, monolayer cultures do not recapitulate the three dimensional context of tumor structures, which can influence cell's response to compounds or compounds administered in vitro may be metabolized to another active (or inactive) compound in vivo. Thus, observations from in vitro promoter studies may not reflect the in vivo modulation of the promoter.

Determining gene promoter regulation in vivo is quite challenging. Recent advances in BLI have allowed for the ability to identify activation of gene promoters in mice genetically modified to express lux driven by either a constitutive or inducible promoter [27]. However, evaluation of promoter activation within cancer cells growing in bone in vivo has not been described. The current study was primarily designed to develop a method to identify gene promoter regulation in vivo in intraosseous tumor cells. Accordingly, in the current study, we evaluated the known activating effects of VitD on the RANKL promoter [26] as well as determining if TGF- β induced RANKL promoter in vitro, thus setting the groundwork for in vivo evaluation. Our observation that VitD and TGF- β induced the RANKL promoter in vivo was supported by the observation that RANKL mRNA levels in the tumors paralleled the BLI results. Finally, the demonstration that lux was present in the CaP cells in the bone confirmed the origin of the lux. Taken together, these

results demonstrate that BLI is a sound method for measuring promoter activation in bone in vivo.

Monitoring tumor growth in bone metastases models has been a great challenge due to the inaccessibility of the bone. Typically measurement is made using radiographs. However, radiographs have several drawbacks, including (1) lack of sensitivity as over 50% of the bone mineral density has to change prior to it being detected as a change on radiographs; (2) they only provide a one dimensional evaluation of the bone and do not allow quantitative determination of total tumor volume; and (3) they are an indirect measure of the tumor, specifically as they only identify the effect of tumor on bone, not the tumor itself. Thus, results from the current study indicate that BLI may have advantages over radiographic imaging of bone tumors and suggest that it is a valuable method for measuring intraosseous tumor growth. The observation that BLI measurement of tumor burden paralleled PSA levels provides a strong level of confidence in the BLI quantification of tumor burden. However, in addition to quantifying tumor burden levels, tumor localization is an advantage that BLI offers over measurement of PSA. In addition to intraosseous growth, we have found that BLI can be used to measure subcutaneous and orthotopic CaP growth of stably-transfected C4-2B, as well as DU145 and PC-3 CaP cells (data not shown) similar to its ability to be useful for measuring response of brain tumors to chemotherapeutic treatment in rodents [25]. The subcutaneous tumors demonstrated a higher basal level of lux compared to the bone tumors and a similar induction of the promoter with treatment. It is unclear if the higher basal lux levels observed in the subcutaneous tumors was due to microenvironment effects (i.e., bone vs. subcutaneous sites) or due to the fact that the subcutaneous-derived signal did not need to penetrate bone or that there was more tumor mass in the subcutaneous tumors.

Several methods of non-invasive imaging of animal cancer models have been developed (reviewed in Ref. 28). Micro-positron emission tomography (Micro-PET) has been used to identify uptake of systemically and intratumorally administered reporter virus in a variety of cancer cells (reviewed in Ref. 29) including CaP cells xenografts in mice [30]. Micro-PET could identify the tumors; however, significant systemic transgene leakage occurred resulting in significant hepatic expression of reporter. This contrasts with the current study in which lux expression is maintained at the site of tumor cells. Regardless, the MicroPET method offers the potential of being able to track gene therapy in clinical cases. In another study [31], demonstrated the ability to detect adenoviral-mediated lux expression was detected in skeletal muscle of mice using a cooled charged coupled device (CCD) camera.

This method demonstrated great sensitivity for detecting lux for a duration of greater than 150 days. Similarly, in the current study, we observed lux activity in tumor cells for an extended period of time (i.e., for 42 days, at which time mice were sacrificed), which demonstrates the utility of this method for longitudinal studies.

Cross-talk between tumor and bone occurs has been postulated to play a major role in the development of CaP bone metastases [1,2]. The basal levels of RANKL promoter activity induced in the C4-2B tumors implanted into bone may have been due to a variety of factors that have been shown to induce RANKL expression including interleukins-1 [32] and -11 [33], parathyroid hormone [34] and TNF [33]. When CaP cells grow in bone, they induce bone resorption, which results in release of many bone ECM factors, including TGF- β [22]. TGF- β signals through TGF β -I and TGF β -II receptors which have been identified in normal as well as in cancerous human and animal prostate cells [35,36]. However, expression of TGF- β receptors in CaP is controversial [37], yet several studies have demonstrated that TGF- β is functional in CaP cells [38–41]. Data from the current manuscript demonstrate that TGF- β activates the RANKL promoter resulting in increased RANKL production, which has been reported to allow the CaP cells to induce osteoclastogenesis and osteoclast activation that results in bone resorption [5]. The resorptive component of CaP has been shown by several studies to be an important component of the establishment of osteoblastic CaP bone metastases [2,6,42]. Thus, results from the current study suggest that CaP-induce bone resorption, which releases TGF- β , will further enhance RANKL production and more bone resorption in a vicious cycle. However, due to the overall osteoblastic nature of CaP, there must be regulation of this osteoclastogenic activity. One possible regulator of this activity is OPG, an inhibitor of RANKL, which is produced by CaP cells [10,43,44] and is elevated in the serum of men with CaP [45].

In conclusion, we described a method to measure CaP tumor growth in bone over time and a novel method for determination of promoter activation within formed CaP tumors in the bone microenvironment *in vivo*. Using the latter method, we determined that TGF- β induces RANKL expression through activation of the RANKL promoter in CaP in bone. This finding is consistent with the idea the cross-talk between tumor and bone is important in the development of bone metastases [2] and identifies TGF- β as a potential target to regulate the establishment of CaP growth in bone. Additionally, the methodology used to measure promoter activity *in vivo* should be useful for determining the influence of microenvironment

(e.g., bone vs. liver metastatic sites) on gene regulation in cancer cells and can be useful to test the effect on gene promoter modulation of compounds that are metabolized to active forms *in vivo*, which cannot be tested *in vitro*. Finally, this methodology has the potential to be useful for evaluating therapies designed to modulate regulation of cancer relevant genes including monitoring both tumor volume and gene regulation.

REFERENCES

1. Rosol TJ. Pathogenesis of bone metastases: Role of tumor-related proteins. *J Bone Miner Res* 2000;15(5):844–850.
2. Keller ET, Zhang J, Cooper CR, Smith PC, McCauley LK, Pienta KJ, *et al.*^{Q2} Prostate carcinoma skeletal metastases: Cross-talk between tumor and bone. *Cancer Metastasis Rev* 2001;20(3–4):333–349.
3. Charhon SA, Chapuy MC, Delvin EE, Valentin-Opran A, Edouard CM, Meunier PJ. Histomorphometric analysis of sclerotic bone metastases from prostatic carcinoma special reference to osteomalacia. *Cancer* 1983;51(5):918–924.
4. Urwin GH, Percival RC, Harris S, Beneton MN, Williams JL, Kanis JA. Generalised increase in bone resorption in carcinoma of the prostate. *Br J Urol* 1985;57(6):721–723.
5. Zhang J, Dai J, Qi Y, Lin DL, Smith P, Strayhorn C, *et al.*^{Q3} Osteoprotegerin inhibits prostate cancer-induced osteoclastogenesis and prevents prostate tumor growth in the bone. *J Clin Invest* 2001;107(10):1235–1244.
6. Yonou H, Kanomata N, Goya M, Kamijo T, Yokose T, Hasebe T, *et al.*^{Q4} Osteoprotegerin/osteoclastogenesis inhibitory factor decreases human prostate cancer burden in human adult bone implanted into nonobese diabetic/severe combined immunodeficient mice. *Cancer Res* 2003;63(9):2096–2102.
7. Clarke NW, McClure J, George NJ. Disodium pamidronate identifies differential osteoclastic bone resorption in metastatic prostate cancer. *Br J Urol* 1992;69(1):64–70.
8. Burgess TL, Qian Y, Kaufman S, Ring BD, Van G, Capparelli C, *et al.*^{Q5} The ligand for osteoprotegerin (OPGL) directly activates mature osteoclasts. *J Cell Biol* 1999;145(3):527–538.
9. Kostenuik PJ, Shalhoub V. Osteoprotegerin: A physiological and pharmacological inhibitor of bone resorption. *Curr Pharm Des* 2001;7(8):613–635.
10. Brown JM, Corey E, Lee ZD, True LD, Yun TJ, Tondravi M, *et al.*^{Q6} Osteoprotegerin and rank ligand expression in prostate cancer. *Urology* 2001;57(4):611–616.
11. Lee Y, Schwarz E, Davies M, Jo M, Gates J, Wu J, *et al.*^{Q7} Differences in the cytokine profiles associated with prostate cancer cell induced osteoblastic and osteolytic lesions in bone. *J Orthop Res* 2003;21(1):62–72.
12. Kartsogiannis V, Zhou H, Horwood NJ, Thomas RJ, Hards DK, Quinn JM, *et al.*^{Q8} Localization of RANKL (receptor activator of NF kappa B ligand) mRNA and protein in skeletal and extraskelatal tissues. *Bone* 1999;25(5):525–534.
13. Weitzmann MN, Cenci S, Rifas L, Haug J, Dipersio J, Pacifici R. T cell activation induces human osteoclast formation via receptor activator of nuclear factor kappaB ligand-dependent and -independent mechanisms. *J Bone Miner Res* 2001;16(2):328–337.
14. Kotake S, Udagawa N, Hakoda M, Mogi M, Yano K, Tsuda E, *et al.*^{Q9} Activated human T cells directly induce osteoclastogenesis from human monocytes: Possible role of T cells in bone

- destruction in rheumatoid arthritis patients. *Arthritis Rheum* 2001;44(5):1003–1012.
15. Locklin RM, Khosla S, Turner RT, Riggs BL. Mediators of the biphasic responses of bone to intermittent and continuously administered parathyroid hormone. *J Cell Biochem* 2003;89(1):180–190.
 16. Fu Q, Jilka RL, Manolagas SC, O'Brien CA. Parathyroid hormone stimulates receptor activator of NF-kappa B ligand and inhibits osteoprotegerin expression via protein kinase A activation of cAMP-response element-binding protein. *J Biol Chem* 2002;277(50):48868–48875.
 17. Kitazawa R, Kitazawa S, Maeda S. Promoter structure of mouse *RANKL/TRANSC/OPGL/ODF* gene. *Biochim Biophys Acta* 1999;1445(1):134–141.
 18. Collin-Osdoby P, Rothe L, Anderson F, Nelson M, Maloney W, Osdoby P. Receptor activator of NF-kappa B and osteoprotegerin expression by human microvascular endothelial cells, regulation by inflammatory cytokines, and role in human osteoclastogenesis. *J Biol Chem* 2001;276(23):20659–20672.
 19. Palmqvist P, Persson E, Conaway HH, Lerner UH. IL-6, leukemia inhibitory factor, and oncostatin M stimulate bone resorption and regulate the expression of receptor activator of NF-kappa B ligand, osteoprotegerin, and receptor activator of NF-kappa B in mouse calvariae. *J Immunol* 2002;169(6):3353–3362.
 20. Koshihara Y, Hoshi K, Okawara R, Ishibashi H, Yamamoto S, Vitamin K. Stimulates osteoblastogenesis and inhibits osteoclastogenesis in human bone marrow cell culture. *J Endocrinol* 2003;176(3):339–348.
 21. Yan T, Riggs BL, Boyle WJ, Khosla S. Regulation of osteoclastogenesis and RANK expression by TGF-beta1. *J Cell Biochem* 2001;83(2):320–325.
 22. Guise TA. Molecular mechanisms of osteolytic bone metastases. *Cancer* 2000;88(Suppl 12):2892–2898.
 23. Wu TT, Sikes RA, Cui Q, Thalmann GN, Kao C, Murphy CF, et al.^{Q10} Establishing human prostate cancer cell xenografts in bone: Induction of osteoblastic reaction by prostate-specific antigen-producing tumors in athymic and SCID/bg mice using LNCaP and lineage-derived metastatic sublines. *Int J Cancer* 1998;77(6):887–894.
 24. Anderson DM, Maraskovsky E, Billingsley WL, Dougall WC, Tometsko ME, Roux ER, et al.^{Q11} A homologue of the TNF receptor and its ligand enhance T-cell growth and dendritic-cell function. *Nature* 1997;390(6656):175–179.
 25. Rehemtulla A, Stegman LD, Cardozo SJ, Gupta S, Hall DE, Contag CH, et al.^{Q12} Rapid and quantitative assessment of cancer treatment response using in vivo bioluminescence imaging. *Neoplasia* 2000;2(6):491–495.
 26. Kitazawa R, Kitazawa S, Vitamin D(3) augments osteoclastogenesis via vitamin D-responsive element of mouse *RANKL* gene promoter. *Biochem Biophys Res Commun* 2002;290(2):650–655.
 27. Zhang W, Feng JQ, Harris SE, Contag PR, Stevenson DK, Contag CH. Rapid in vivo functional analysis of transgenes in mice using whole body imaging of luciferase expression. *Transgenic Res* 2001;10(5):423–434.
 28. Lewis JS, Achilefu S, Garbow JR, Laforest R, Welch MJ. Small animal imaging: Current technology and perspectives for oncological imaging. *Eur J Cancer* 2002;38(16):2173–2188.
 29. Gambhir SS. Molecular imaging of cancer with positron emission tomography. *Nat Rev Cancer* 2002;2(9):683–693.
 30. Pantuck AJ, Berger F, Zisman A, Nguyen D, Tso CL, Matherly J, et al.^{Q13} CL1-SR39: A noninvasive molecular imaging model of prostate cancer suicide gene therapy using positron emission tomography. *J Urol* 2002;168(3):1193–1198.
 31. Wu JC, Sundaresan G, Iyer M, Gambhir SS. Noninvasive optical imaging of firefly luciferase reporter gene expression in skeletal muscles of living mice. *Mol Ther* 2001;4(4):297–306.
 32. Weitzmann MN, Cenci S, Rifas L, Brown C, Pacifici R. Interleukin-7 stimulates osteoclast formation by up-regulating the T-cell production of soluble osteoclastogenic cytokines. *Blood* 2000;96(5):1873–1878.
 33. Nakashima T, Kobayashi Y, Yamasaki S, Kawakami A, Eguchi K, Sasaki H, et al.^{Q14} Protein expression and functional difference of membrane-bound and soluble receptor activator of NF-kappaB ligand: Modulation of the expression by osteotropic factors and cytokines. *Biochem Biophys Res Commun* 2000;275(3):768–775.
 34. Ma YL, Cain RL, Halladay DL, Yang X, Zeng Q, Miles RR, et al.^{Q15} Catabolic effects of continuous human PTH (1–38) in vivo is associated with sustained stimulation of RANKL and inhibition of osteoprotegerin and gene-associated bone formation. *Endocrinology* 2001;142(9):4047–4054.
 35. Wikstrom P, Lindh G, Bergh A, Damber JE. Alterations of transforming growth factor beta1 (TGF-beta1) and TGFbeta receptor expressions with progression in Dunning rat prostatic adenocarcinoma sublines. *Urol Res* 1999;27(3):185–193.
 36. Wong YC, Xie W, Tsao SW. Structural changes and alteration in expression of TGF-beta1 and its receptors in prostatic intraepithelial neoplasia (PIN) in the ventral prostate of noble rats. *Prostate* 2000;45(4):289–298.
 37. Wikstrom P, Damber J, Bergh A. Role of transforming growth factor-beta1 in prostate cancer. *Microsc Res Tech* 2001;52(4):411–419.
 38. Steiner MS, Wand GS, Barrack ER. Effects of transforming growth factor beta 1 on the adenylyl cyclase-cAMP pathway in prostate cancer. *Growth Factors* 1994;11(4):283–290.
 39. Chipuk JE, Cornelius SC, Pultz NJ, Jorgensen JS, Bonham MJ, Kim SJ, et al.^{Q16} The androgen receptor represses transforming growth factor-beta signaling through interaction with Smad3. *J Biol Chem* 2002;277(2):1240–1248.
 40. Kang HY, Lin HK, Hu YC, Yeh S, Huang KE, Chang C. From transforming growth factor-beta signaling to androgen action: Identification of Smad3 as an androgen receptor coregulator in prostate cancer cells. *Proc Natl Acad Sci USA* 2001;98(6):3018–3023.
 41. Kim IY, Zelner DJ, Lee C. The conventional transforming growth factor-beta (TGF-beta) receptor type I is not required for TGF-beta 1 signaling in a human prostate cancer cell line, LNCaP. *Exp Cell Res* 1998;241:151–160.
 42. Corey E, Brown LG, Quinn JE, Poot M, Roudier MP, Higano CS, et al.^{Q17} Zoledronic acid exhibits inhibitory effects on osteoblastic and osteolytic metastases of prostate cancer. *Clin Cancer Res* 2003;9(1):295–306.
 43. Penno H, Silfversward CJ, Frost A, Brandstrom H, Nilsson O, Ljunggren O. Osteoprotegerin secretion from prostate cancer is stimulated by cytokines, in vitro. *Biochem Biophys Res Commun* 2002;293(1):451–455.
 44. Holen I, Croucher PJ, Hamdy FC, Eaton CL. Osteoprotegerin (OPG) is a survival factor for human prostate cancer cells. *Cancer Res* 2002;62(6):1619–1623.
 45. Brown JM, Vessella RL, Kostenuik PJ, Dunstan CR, Lange PH, Corey E. Serum osteoprotegerin levels are increased in patients with advanced prostate cancer. *Clin Cancer Res* 2001;7(10):2977–2983.